

Synthesis and Structure–Activity Relationship Studies of Small Molecule Disruptors of EWS-FLI1 Interactions in Ewing's Sarcoma

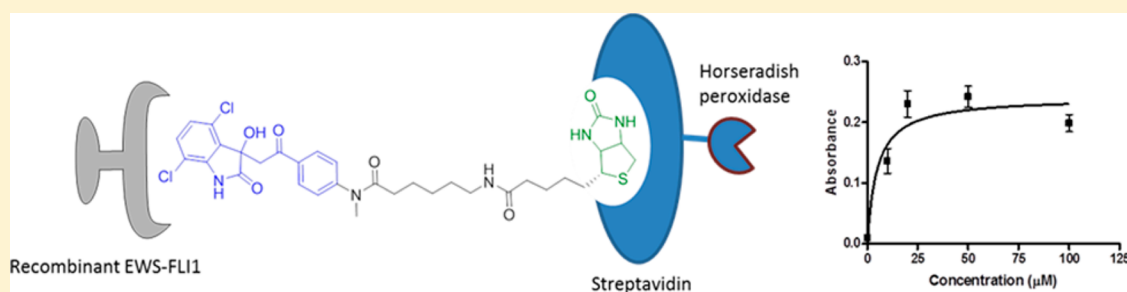
Perrer N. Tosso,^{†,‡,§} Yali Kong,^{†,§} Lauren Scher,[§] Ryan Cummins,[§] Jeffrey Schneider,[§] Said Rahim,[§] K. Travis Holman,^{||} Jeffrey Toretzky,[§] Kan Wang,[†] Aykut Üren,[§] and Milton L. Brown^{*,†,§}

[†]Center for Drug Discovery, Georgetown University Medical Center, New Research Building EP07, 3970 Reservoir Road, NW, Washington, D.C. 20057, United States

[‡]Department of Biochemistry and Molecular Biology, Georgetown University Medical Center, Washington, D.C. 20057, United States

[§]Lombardi Comprehensive Cancer Center, Georgetown University Medical Center, New Research Building, 3970 Reservoir Road, NW, Washington, D.C. 20057, United States

^{||}Department of Chemistry, Georgetown University, 37th and O Streets, NW, Washington D.C 20057, United States



ABSTRACT: EWS-FLI1 is an oncogenic fusion protein implicated in the development of Ewing's sarcoma family tumors (ESFT). Using our previously reported lead compound **2** (YK-4-279), we designed and synthesized a focused library of analogues. The functional inhibition of the analogues was measured by an EWS-FLI1/NROB1 reporter luciferase assay and a paired cell screening approach measuring effects on growth inhibition for human cells containing EWS-FLI1 (TC32 and TC71) and control PANC1 cell lines devoid of the oncoprotein. Our data revealed that substitution of electron donating groups at the para-position on the phenyl ring was the most favorable for inhibition of EWS-FLI1 by analogs of **2**. Compound **9u** (with a dimethylamino substitution) was the most active inhibitor with $GI_{50} = 0.26 \pm 0.1 \mu\text{M}$. Further, a correlation of growth inhibition (EWS-FLI1 expressing TC32 cells) and the luciferase reporter activity was established ($R^2 = 0.84$). Finally, we designed and synthesized a biotinylated analogue and determined the binding affinity for recombinant EWS-FLI1 ($K_d = 4.8 \pm 2.6 \mu\text{M}$).

INTRODUCTION

Ewing's sarcoma (ES) is a malignant tumor in adolescents and young adults¹ and presents a high propensity for metastasis, particularly to lung, bone, and bone marrow. ES is an orphan disease with more than 200 new cases diagnosed in the United States each year. ES arises from the mesenchymal tissues occurring mostly in the bones; however, approximately 10% of the tumors arise in the soft tissues of the chest wall, pelvis, and leg.^{2–4} Currently, adjuvant therapy is required to treat both the primary tumor and the presumed microscopic metastasis. The intensive combination of chemotherapy, surgery, and radiation has increased the disease-free survival rate to 70% in patients with localized ES. Patients with metastatic ES have a poor prognosis,⁵ and thus, the development of specific therapeutic agents targeting ES is urgently needed.

ES is characterized by a nonrandom balanced chromosomal translocation involving the EWS gene and one of the several ETS family of transcription factor genes, mainly FLI1,⁶ resulting in the oncoprotein EWS-FLI1. The most common

translocation in ES is the t(11;22)(q24;q12) translocation and occurs in 90–95% of ES cases. The high frequency of this translocation suggest that the product plays a significant role in the origin of these malignancies.⁷

EWS-FLI1 consists of the N-terminal RNA-binding domain of EWS and the C-terminal DNA-binding domain of transcription factors such as ETS family.^{8,9} During this fusion, the transactivation domain of FLI1 is replaced by the N-terminal region of EWS converting FLI1 into an oncoprotein. Elimination of EWS-FLI1 through small interfering and antisense RNA results in the prolonged survival of ES xenograft-bearing mice.¹⁰ Consequently, this oncoprotein may provide a unique target in the development of therapeutics against ES.

EWS-FLI1 is predicted to be an intrinsically disordered protein (IDP), i.e., lacks secondary and tertiary structure under

Received: May 15, 2014

Published: November 28, 2014

physiological conditions.¹¹ The disordered nature of EWS-FLI1 is necessary for optimal transactivation of transcription¹² and the formation of the protein–protein complexes that lead to oncogenesis.¹³ Targeting transcription factors requires either the disruption of specific DNA–protein or protein–protein interactions.¹⁴ However, because of their higher induced-fit sampling properties, IDPs have potential for binding to small molecules and may possess potentially multiple binding sites for small molecules.¹⁵

We previously reported the discovery of NSC635437 (**1**), identified through screening of small molecules against recombinant EWS-FLI1 using surface plasmon resonance, and we developed YK-4-279 (**2**) with limited SAR (Figure 1A).

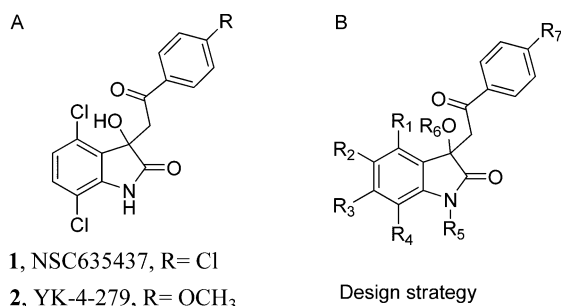


Figure 1. (A) Structures of EWS-FLI1 inhibitors: **1** = NSC635437, GI_{50} = 20 μ M in TC32 cells; **2** = YK-4-279, K_d = 9.48 μ M, GI_{50} of 0.5–2.0 μ M in several ES cells. (B) Sites for modifications.

Both compounds bind EWS-FLI1 and disrupt EWS-FLI1/RHA interaction.^{16,17} We have shown that **2** specifically and stereoselectively¹⁸ inhibits the function EWS-FLI1 and induces apoptosis both in vitro (GI_{50} = 0.5–2.0 μ M in ES cells) and in vivo.¹⁷

In this study, we report the full SAR studies of **2** against two Ewing's sarcoma cell lines (TC32 and TC71) and the transcriptional inhibition of EWS-FLI1. Finally, we designed and synthesized a novel biotinylated analogue of an active inhibitor to measure binding affinity to EWS-FLI1.

CHEMISTRY

Our previous study led to the discovery of compound **1** (Figure 1), 4,7-dichloro-3-(2-(4-chlorophenyl)-2-oxoethyl)-3-hydroxyindolin-2-one, which displayed antiproliferative activity against various ES cell lines with GI_{50} of 20 μ M in TC32 cells.¹⁷ The aromatic *p*-methoxy substitution on the phenyl ring afforded compound **2** which exhibited an increased activity with GI_{50} of 0.9 μ M in TC32 cells.¹⁷

Since EWS-FLI1 is more than 75% disordered,¹⁹ a lack of crystal structure or homology model of the protein²⁰ requires a ligand based approach. Thus, we designed a patterned structural study of **2** to obtain structure–activity information and to investigate the electrostatic, steric, and hydrogen bonding requirements for inhibition.

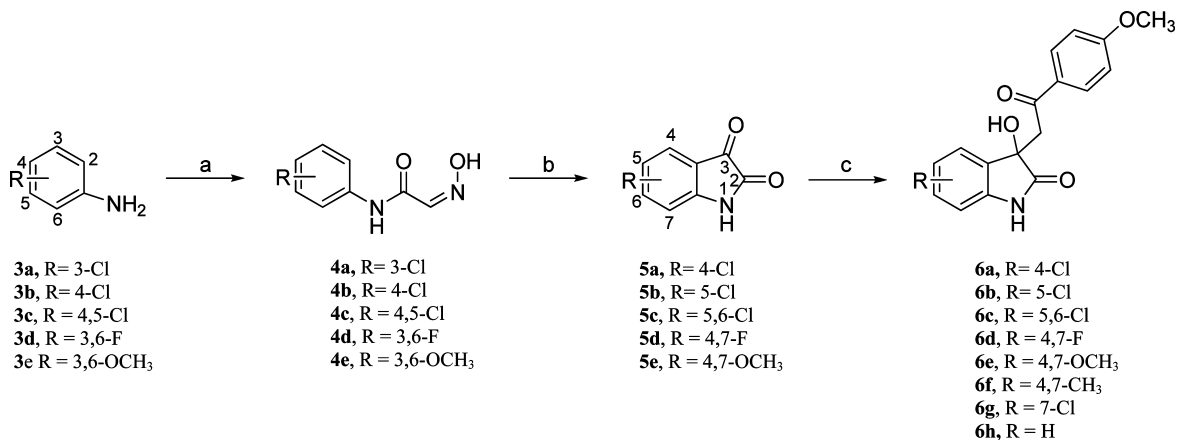
To explore the importance of the 4,7-dichloro substituent group on the indoline ring of **2**, we synthesized indolin-2-one substituted compounds **6a–h** (Scheme 1). A corresponding aniline (**3a–e**) was reacted with chloral hydrate and hydroxylamine hydrochloride in aqueous sodium sulfate to form isonitrosoacetanilide (**4a–e**) followed by a Sandmeyer reaction with concentrated sulfuric acid to afford the desired isatin (**5a–e**) in good yield (55–90%).^{21,22} We observed that maintaining the temperature at 55 °C is necessary for the synthesis of the 4,7-difluoro and 4,7-dimethoxy substituted intermediates. Isatins **5f–h** were commercially available, and the aldol reaction was performed in methanol (with Et_2NH as a catalyst) to give **6a–h** in excellent yield (90–100%).

The synthetic strategy for substituting the phenyl ring of **2** is shown in Scheme 2. In general, commercially available 4,7-dichloroisatin was condensed with a substituted acetophenone (**8a–u**) in the presence of a catalytic amount of Et_2NH to afford **9a–u** in excellent yield (90–100%).²³

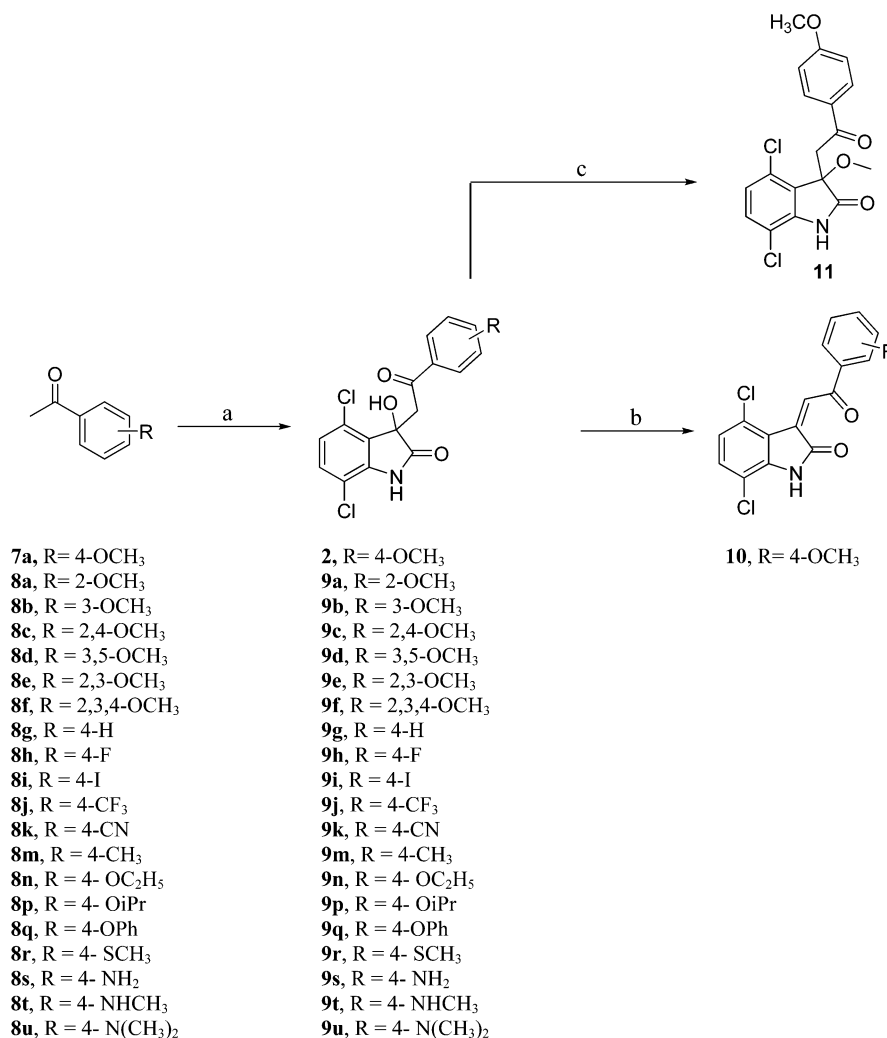
To understand the importance of the hydroxyl group in the aldol product and to assess the potential for an in vivo dehydration reaction, we synthesized the dehydrated compound **10**. This was accomplished by treating **2** with concentrated sulfuric acid as shown in Scheme 2 (58% yield).^{23,24} Of interest was the report that this methodology affords the *Z* isomer.²⁴ We confirmed and assigned the *Z* configuration of **10** by X-ray crystallography (Figure 2).

Hydrogen bonding has an important role in ligand receptor interactions.²⁵ To check the involvement of the indoline

Scheme 1^a



^aReagents and conditions: (a) $Cl_3CCH(OH)_2$, $NH_2OH \cdot HCl$, Na_2SO_4 , H_2O , HCl , 55 °C, overnight; (b) H_2SO_4 , 55–80 °C, (c) 4-methoxyacetophenone, Et_2NH , MeOH, rt, 90–100%.

Scheme 2^a

^aReagents and conditions: (a) 4,7-dichloroisatin, Et₂NH, MeOH, rt, 90–100%; (b) H₂SO₄, 0 °C, 5 min, 58%; (c) Ag₂O, THF, MeI, rt, 58%.

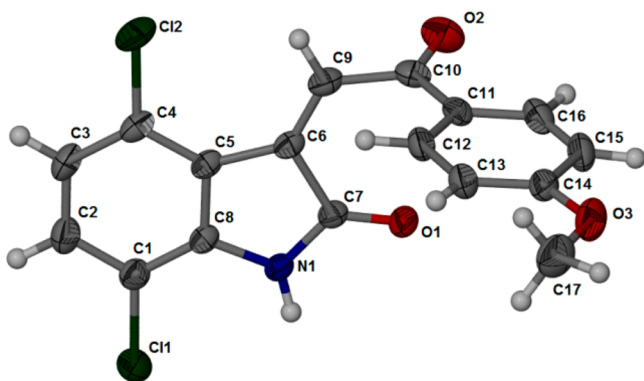


Figure 2. X-ray single crystal structure of **10**, the dehydration product of **2**. The structure determination establishes the *Z* stereochemistry of **10**.

hydroxyl and amine group in potential hydrogen bonding, we synthesized the methylated compounds **11**, **14a,b**, and **15**. Compound **11** was synthesized through the O-methylation of **2** by treating the aldol with methyl iodine in silver oxide to afford **11** with a yield of 58% (Scheme 2).²⁶ Compound **14a** was synthesized by N-methylating the isatin (Scheme 3). The

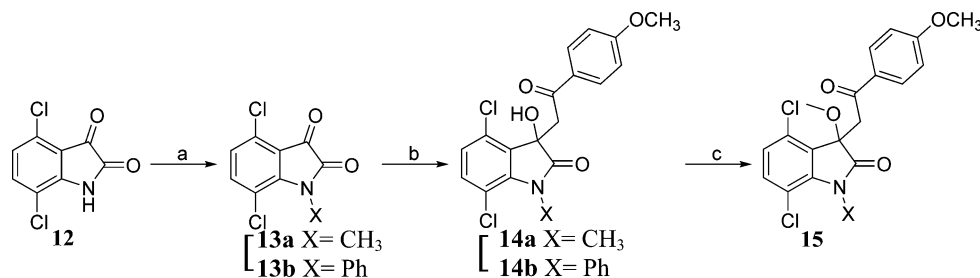
double methylated compound **15** was obtained by treating **14a** with methyl iodine in silver oxide.

We synthesized analog **18** with a pyridine ring instead of the phenyl ring in an attempt to increase the solubility of the lead compound. The synthesis of **18** began with a bromine–lithium exchange in the reaction of **16** with acetaldehyde in the presence of *n*-BuLi. The resulting alcohol was oxidized in PDC and 4 Å molecular sieves to afford **17**. Reaction of **17** with 4,7-dichloroisatin afforded the desired compound **18** in 90% yield (Scheme 4).

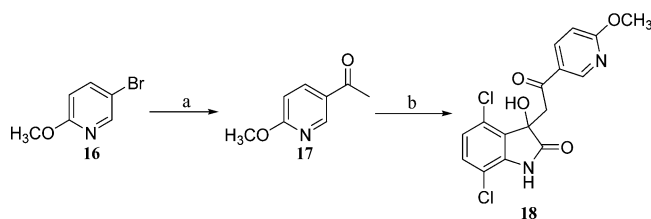
To further assess binding affinity of these derivatives with EWS-FLI1, we synthesized a biotin conjugate of **9t** (Scheme 5). The synthesis started with the Boc (*tert*-butoxycarbonyl) protection of the 5-aminopentanoic acid (**19**) followed by coupling with 4-acetyl-*N*-methylaniline with DCC to give **21**. An aldol addition of **21** with 4,7-dichloroisatin yielded **22** followed by its deprotection to afford **23**. EDCI coupling of biotin to **23** provided the final biotin conjugate analogue **24** in 49% yield.

RESULTS AND DISCUSSION

The antiproliferative properties of the derivatives were assayed by monitoring their ability to inhibit cell growth using a water-

Scheme 3^a

^aReagents and conditions: (a) NaH, MeI, DMF, 0 °C to rt, 54.5%; (b) 4-methoxyacetophenone, Et₂NH, MeOH, rt, 51–100%; (c) Ag₂O, THF, MeI, rt, 56%.

Scheme 4^a

^aReagents and conditions: (a) (1) acetaldehyde, *n*-BuLi, THF, –78 °C; (2) PDC, 4 Å molecular sieves, CH₂Cl₂, 0 °C; (b) 4,7-dichloroisatin, Et₂NH, MeOH, rt, 90%.

soluble tetrazolium (WST) assay (see Experimental Section). Antiproliferative activities of the small molecules were determined as described in the Experimental Section in the two human ES cell lines (TC32 and TC71) and their GI₅₀ values were evaluated. The results are summarized in Tables 1–4. Compound **2** was used as comparison in the parallel experiments.

Compounds **6a–h** were synthesized to investigate the importance of different substituent groups in the indoline ring as compared to **2** (Table 1). Of all the compounds in this series, only the dimethoxy substituted compound (**6e**) retained the same potency as **2** (GI₅₀ = 1.0 μM) in TC32 cells. Since both electron withdrawing (–Cl) and donating group substitutions (–OCH₃) in the R₁ and R₄ positions were active, differences in steric contributions were considered. Increased size of the aromatic substitution in the R₁ and R₄ positions (compound **6d** versus **2**) appears to contribute to improved inhibitory activity. Because **6e** does not significantly improve the pharmacological properties of **2**, we kept the 4,7-dichloro substitutions on the indoline ring for the rest of our study.

Compound **2** contains a chiral center. In a previous study, we found that the *S*-(-) was 4-fold (GI₅₀ = 0.28 μM) more potent in vitro than the racemic **2**. The *R*-(+) was almost inactive in vitro.¹⁸ To further understand the influence of the hydroxyl group and the potential dehydration in vivo, we synthesized the dehydrated analog of **2**. The dehydrated compound **10** was as potent as the parent compound **2** (GI₅₀ = 1.0 μM in TC32), suggesting that the hydroxyl group is not required for binding. We prepared derivative **11** in which the hydroxyl group was methylated to eliminate potential hydrogen bond donation. This chemical transformation resulted in a complete loss of inhibitory activity. Further methylations performed are summarized in Table 2. The methylation of the amide group, represented by compound **14a**, resulted in a 2-fold reduction in TC32 cell GI₅₀. Furthermore, the replacement of the proton on

the amide with a phenyl group (**14b**) resulted in the complete loss of activity apparently due to steric effects. The *O*-methylated and *N*-methylated compound **15** was inactive.

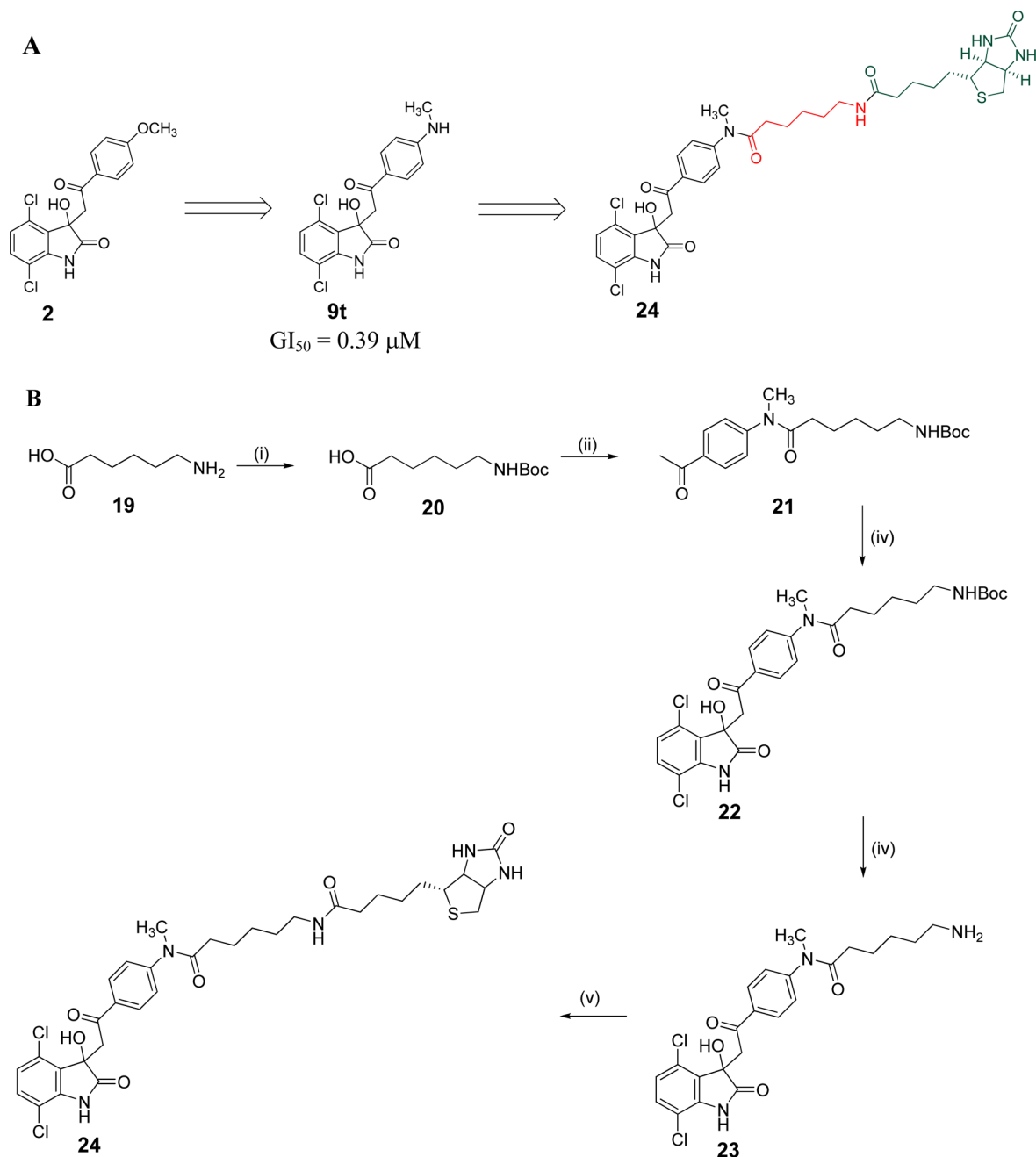
As previously described, we synthesized **18** by replacing the electron rich phenyl ring by an electron deficient pyridine ring. This resulted in a complete loss of growth inhibition for the EWS-FLI1 containing cells lines (data not shown).

We further evaluated the positional effect of the methoxy moiety on the phenyl ring, and the results are summarized in Table 3. The data showed that substitution with 2-methoxy, 3-methoxy, and the 2,3-methoxy (**9a**, **9b**, and **9e**) reduced inhibition of cell growth. The 3,5-dimethoxy derivative **9d** also resulted in a nearly 10-fold loss of growth activity in TC32 cells. Interestingly, the 2,4-dimethoxy substitution (**9c**) resulted in a GI₅₀ of 2.6 μM, but the 2,3,4-trimethoxy derivative (**9f**) resulted in a 3-fold loss of the growth activity as compared to **2**. Taken together, these data suggested that the para position contributes more to the potency whereas the meta and ortho substitutions decrease the inhibitory activity. We concluded that the mono substitution at the para position on the aromatic ring plays a significant role in the inhibition of EWS-FLI1 in ES cells.

Further SAR studies of the para position on the phenyl ring were performed (**9g–u**) and the results are summarized in Table 4. We found that a substitution of 4-methoxy with electron withdrawing groups (**9h–k**) resulted in the loss of activity. The 4-fluoromethyl derivative (**9j**) displayed a 3-fold loss of inhibitory activity in TC32. However, it should be noted that **9j** also inhibited PANC1 cells growth, suggesting that its inhibitory action was not selective. Thus, **9j** could have generalized off-target toxicity.

The 4-isopropyl substitution **9p** and the bulky phenyl substitution represented by **9q** resulted in the complete loss of activity. Also, the 4-methyl derivative (**9n**) resulted in a complete loss of activity. The 4-ethoxy derivative **9m** displayed a 3-fold decrease of potency in the ES cells, suggesting that substitution with the larger group may be unfavorable to the inhibitory activity of the derivatives. Interestingly, the thiomethyl derivative **9r** retained activity comparable to **2** (GI₅₀ of 0.98 μM). The 4-amine substitution **9s** on the aromatic ring resulted in the complete loss of activity. However, the methylamine derivative **9t** resulted in more than 2-fold increase in potency (GI₅₀ = 0.34 μM) compared to **2** (GI₅₀ = 0.92 μM). The activity was also improved with the dimethylamine derivative **9u** with GI₅₀ of 0.26 μM in TC32 cells. This activity was equal to the potency of the *S*-(-) enantiomer of **2** (GI₅₀ = 0.28 μM) in TC32 cells.¹⁸ Antiproliferative results in TC32 cells were comparable to those observed in TC71 cells.

Functional Inhibition of EWS-FLI1. Previously, we have demonstrated that compound **2** acted as a functional inhibitor

Scheme 5. Design Strategy of the Biotinylated Compound 24^a

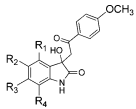
^aReagents and conditions (i) $(\text{Boc})_2\text{O}$, Et_3N , MeOH , 60°C , overnight, 90%; (ii) 4-acetyl-N-methylaniline, DCC, DMAP, CH_2Cl_2 , 0°C to rt, 58%; (iii) 4,7-dichloroisatin, Et_2NH , MeOH , rt, 95%; (iv) 3:1 $\text{CH}_2\text{Cl}_2/\text{TFA}$, rt, 1.5 h; (v) biotin, EDCI-HCl, DMAP, HOBT, CH_2Cl_2 , 0°C to rt, 49%.

of EWS-FLI1.¹⁷ It has been reported that EWS-FLI1 binds directly to the microsatellite repeats of the promoter NROB1 to drive oncogenesis in ES.²⁷ In this study, COS7 cells were transfected with EWS-FLI1 and NROB1 reporter-luciferase plasmids as previously reported (Figure 3A).^{17,28} EWS-FLI1-transfected cells showed a dose-dependent decrease in the promoter activity when treated for 20 h with compound 2 ($\text{IC}_{50} = 0.35 \mu\text{M}$) as compared to no transfection (Figure 3B,C). Control experiments at 48 h show that the compounds were not cytotoxic to the COS7 cells. COS7 are fibroblast-like cells derived from monkey kidney that are devoid of the EWS-FLI1.

To further assess their inhibitory effects on the transcriptional activities of EWS-FLI1, we selected 6e, 9c, 9m, 9r, 9t, 9u,

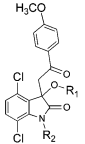
10, and 14a, which displayed a GI_{50} of $2.7 \mu\text{M}$ or better, and 9a, 11, and 15, which displayed no antiproliferative activity (Figure 4A,B). As expected, 9a which displayed no inhibition on cell growth did not inhibit the transcriptional activities of EWS-FLI1. 9r inhibition was comparable to 2 with IC_{50} of $0.33 \mu\text{M}$, whereas 6e has an IC_{50} of $0.77 \mu\text{M}$. Compounds 9c and 9m inhibitory effects were lower than 2. Unlike 11 that did not display any inhibition, 14a and 15 showed modest inhibitory effects on the transcriptional activities of EWS-FLI1. Consistent with the ES cell growth inhibition data, 9t and 9u exhibited better inhibition of EWS-FLI1 with an IC_{50} of 0.18 and $0.15 \mu\text{M}$, respectively. The results strongly support that these derivatives inhibit the transcriptional activity of EWS-FLI1.

Table 1. Chemical Structure and Biological Activities of Compounds 6a–i

	Substitutions				GI ₅₀ (μM)		
	R ₁	R ₂	R ₃	R ₄	PANC 1	TC32	TC71
	-Cl	-H	-H	-H	NI ^a	NI	NI
6b	-Cl	-Cl	H	-H	NI	NI	NI
6c	-H	-Cl	-Cl	-H	NI	NI	NI
6d	-F	-H	-H	-F	NI	NI	NI
6e	-OCH ₃	-H	-H	-OCH ₃	NI	1.0 ^b	0.94 ^b
6f	-CH ₃	-H	-H	-CH ₃	NI	NI	NI
6g	-H	-H	-H	-Cl	NI	NI	NI
6h	-H	-H	-H	-H	NI	NI	NI

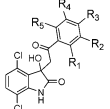
^aNI: no significant inhibition (GI₅₀ > 10 μM). ^bExperimental error is within 20%.

Table 2. Chemical Structure and Biological Activities of O-Methylation and N-Methylation

	Substitutions			GI ₅₀ (μM)		
	R ₁	R ₂	PANC 1	TC32 ^b	TC71 ^b	
	H	H	NI ^a	0.94	0.92	
11	-CH ₃	H	NI	NI	NI	
14a	H	-CH ₃	NI	2.2	0.71	
14b	H	-Ph	NI	NI	NI	
15	-CH ₃	-CH ₃	NI	NI	NI	

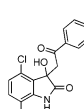
^aNI: no significant inhibition (GI₅₀ > 10 μM). ^bExperimental error is within 20%.

Table 3. Chemical Structure and Biological Activities of Compounds 9a–f

	Substitutions				GI ₅₀ (μM)		
	R ₁	R ₂	R ₃	R ₄	PANC 1	TC32 ^b	TC71 ^b
	H	H	OCH ₃	H	NI*	0.94	0.92
9a	OCH ₃	H	H	H	NI	NI	NI
9b	H	OCH ₃	H	H	NI	NI	NI
9c	OCH ₃	H	OCH ₃	H	NI	2.6	2.8
9d	H	OCH ₃	H	OCH ₃	NI	9.0	NI
9e	OCH ₃	OCH ₃	H	H	NI	NI	NI
9f	OCH ₃	OCH ₃	OCH ₃	H	NI	2.70	4.4

^aNI: no significant inhibition (GI₅₀ > 10 μM). ^bExperimental error is within 20%.

Table 4. Chemical Structure and Biological Activities of Compounds 9g–u

	Substitution		GI ₅₀ (μM) ^{a,b}		
	R ₁	PANC 1	TC32	TC71	
	-OCH ₃	NI	0.94 (0.18)	0.92 (0.12)	
9g	-H	NI	NI	NI	
9h	-F	NI	NI	NI	
9i	-I	NI	NI	NI	
9j	-CF ₃	11.0 (0.23)	2.9 (0.23)	6.9 (0.19)	
9k	-CN	NI	NI	NI	
9n	-CH ₃	NI	NI	NI	
9m	-OC ₂ H ₅	NI	2.70 (0.21)	3.57 (0.19)	
9p	-OiPr	NI	NI	NI	
9q	-OPh	NI	NI	NI	
9r	-SCH ₃	NI	0.98 (0.17)	0.91 (0.14)	
9s	-NH ₂	NI	NI	NI	
9t	-NHCH ₃	NI	0.34 (0.09)	0.39 (0.10)	
9u	-N(CH ₃) ₂	NI	0.26 (0.1)	0.40 (0.07)	

^aNI: no significant inhibition (GI₅₀ > 10 μM). ^bExperimental error represents SEM.

A plot of the IC₅₀ of the luciferase activity versus the GI₅₀ (Figure 5) was performed to show that the cellular growth inhibition effects of the ES cells observed are dependent on the inhibition of the transcriptional activity of EWS-FLI1. A correlation coefficient of 0.84 provides further evidence that the effects on the inhibition of the transcriptional activity of EWS-FLI1 and the cell growth inhibition of ES cells are related. These data suggested that the EWS-FLI1 mediated growth of the ES cells can be effectively decreased by inhibiting the transcriptional activity of EWS-FLI1.

Design and Evaluation of Biotinylated Probe of Compound 24. We envisioned the synthesis of a biotin conjugate that could be used to detect binding of the derivative and the recombinant EWS-FLI1 (Scheme 5A). We developed a synthetic route to append a five-carbon linker terminating with an amine to compound 9t. The amine was exploited to link biotin to the 9t linker molecule to afford 24 (Scheme 5A). We evaluated the binding of 24 to recombinant EWS-FLI1 as shown in Figure 6A. A 96-well plate was coated with the recombinant protein that was allowed to bind with the biotinylated conjugate. The binding of 24 to EWS-FLI1 was detected with HRP streptavidin conjugate. We detected a dose dependent binding of 24 to immobilized EWS-FLI1 (Figure 6B). No binding was detected when BSA was immobilized. The saturation was reached at 20 μM. Concentration-dependent binding of 24 to immobilized EWS-FLI1 (Figure 6B) was exhibited by biotinylated 24 over a range of 1–100 μM, resulting in a K_d of 4.8 ± 2.6 μM.

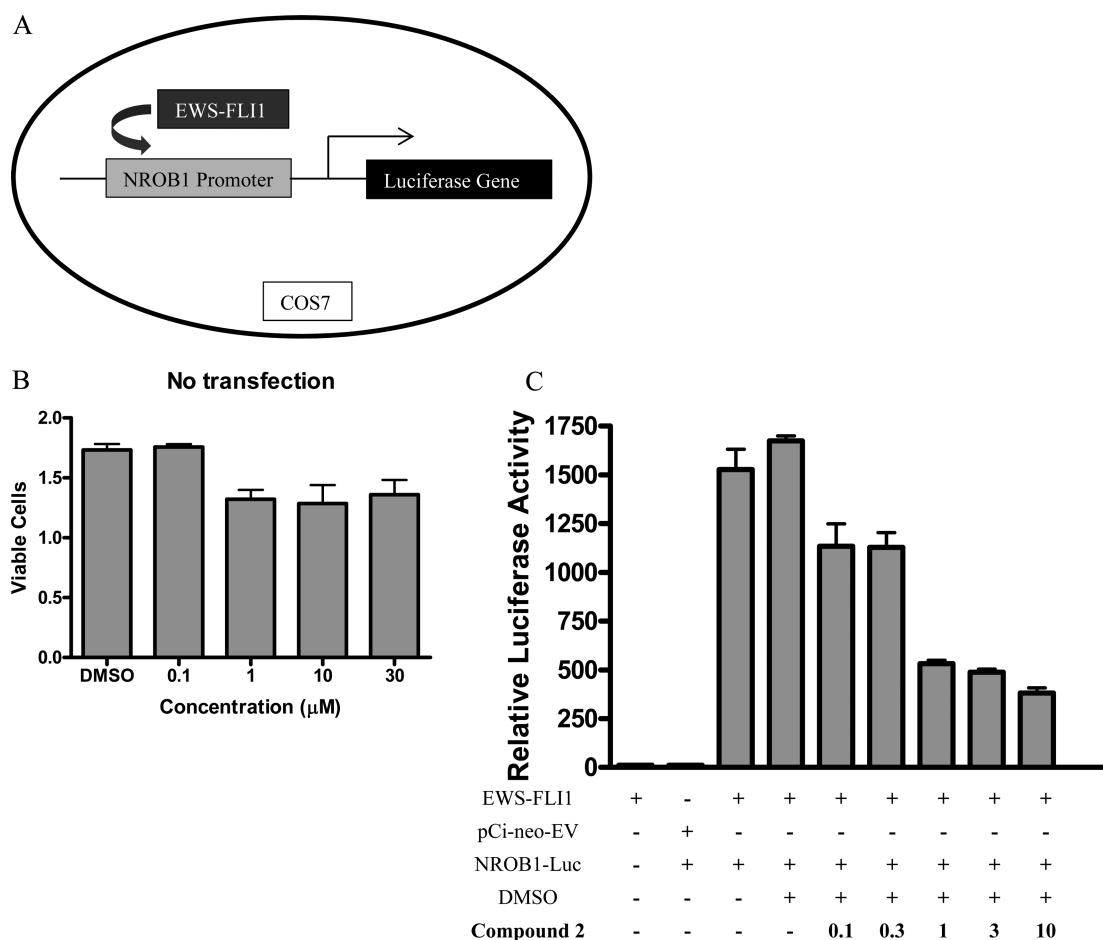


Figure 3. (A) Schematic construct of the luciferase reporter assay for the transcription inhibition of the EWS-FLI1 by small molecule. (B) Cell proliferation assay (WST) indicating negligible effect of compound **2** on COS7 cells. (C) COS7 cells were transfected with NROB1 luciferase reporter and empty vector (pCi-neo-EV) or full length EWS-FLI1. Diagram shows a mean \pm SD of a single representative experiment performed in quadruplicate.

CONCLUSION

This research provides a solid ground for the discovery of new and effective agents to treat Ewing's sarcoma. The hit compound **1** was discovered through a surface plasmon resonance initial screening against recombinant EWS-FLI1. Compound **2** with increased activity reduces the growth of ES cells and ES orthotopic xenografts.¹⁷ Compound **2** was used as our lead compound for further detailed SAR studies.

We modified **2** with the aim to clarify the relevant structural determinants for small molecule inhibition of EWS-FLI1. On the indoline of **2**, our investigation highlights the importance of the 4,7-position and the significance of the free amine for optimal inhibition. We found that removal of the alcohol by dehydration shows that the hydroxyl group is not required for binding. The loss of activity resulting from the removal of hydrogen bond donation supports the finding that the alcohol group does not act as a hydrogen bond donor.

Additionally, we have observed that the para-position on the phenyl ring was the most favorable for inhibition of EWS-FLI1 by **2**. Electron donating groups at the para-position significantly contribute to a higher inhibitory activity. Compounds **9t** and **9u** had over 3-fold higher potency than the lead **2**. It appears that the electron density of the substitutions may play a more significant role in the inhibitory action of the derivatives. The electron density of 4-dimethylamine > 4-methylamine >

4-methoxy correlates with increasing inhibitory activity (compound **9u** > compound **9t** > compound **2**).

We have successfully correlated the cell growth inhibition of the ES cells by the active derivatives with the luciferase reporter activity, statistically linking observed activity to the inhibition of the transcriptional activity of EWS-FLI1. Finally, we showed that a derivative binds to the target using a novel biotin conjugate. The conjugate can be utilized as a screening tool to better understand the binding of small molecules to the EWS-FLI1.

EXPERIMENTAL SECTION

Chemistry. General Chemistry Methods. All solvents and reagents were used as obtained from commercial sources unless otherwise indicated. Commercial reagents and anhydrous solvents were used without further purification. Analytical thin layer chromatography (TLC) was performed on silica gel 60 F254 aluminum sheets. Removal of solvents was conducted by using a rotary evaporator, and residual of solvents was removed from nonvolatile compounds using a vacuum manifold. All reported yields are isolated yields. ¹H and ¹³C NMR spectra were recorded on a Varian 400MR spectrometer operating at 400 MHz for ¹H and 100 MHz for ¹³C. Deuterated dimethyl sulfoxide or deuterated methanol or deuterated chloroform was used as the solvent for NMR experiments. ¹H chemical shift values (δ) are referenced to the residual nondeuterated components of the NMR solvents (δ = 2.54 ppm for DMSO, δ = 7.26 ppm for CDCl₃, and δ = 3.31 ppm for

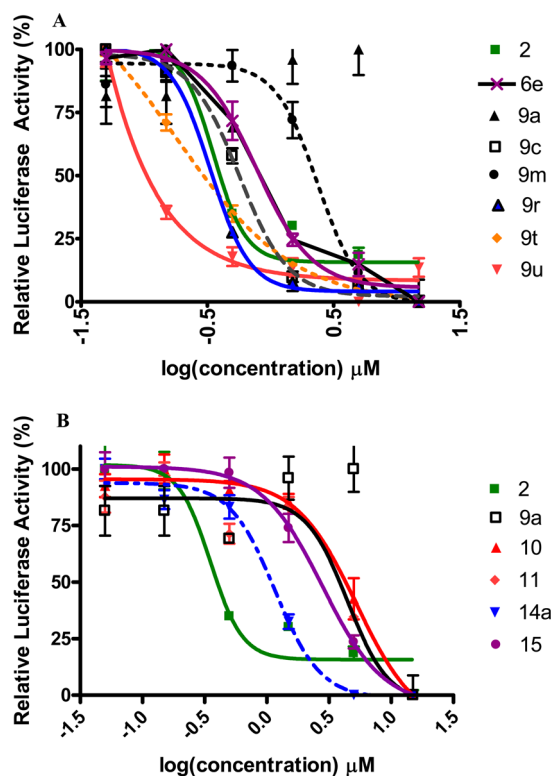


Figure 4. Luciferase assay showing inhibition of EWS-FLI1 transcriptional activity in COS7 cells. (A) Dose–response profiles of compounds 2, 6e, 9a, 9c, 9m, 9r, 9t, 9u for EWS-FLI1 inhibition. (B) Dose–response profiles of compounds 2, 9a, 10, 11, 14a, 15 for EWS-FLI1 inhibition. Diagrams show a mean \pm SD of single representative experiment performed in quadruplicate, with compound 2 graphed in comparison and 9a as negative control.

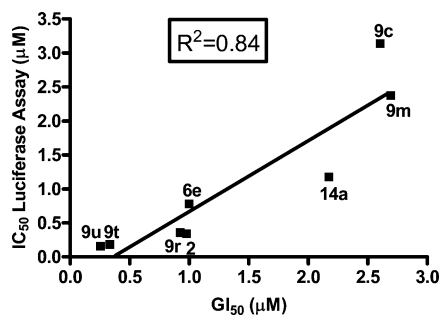


Figure 5. Correlation of the analogs on growth inhibition in TC32 cells and luciferase reporter activity in COS7 cells.

CD₃OD). The ¹³C chemical shifts (δ) are referenced to CDCl₃ (central peak, δ = 77.16 ppm) or CD₃OD (δ = 49.00 ppm) as the internal standard. The HRMS data were obtained on a Waters Q-TOF Premier mass spectrometer. Column chromatography was performed using silica gel (35–75 mesh). The purity of final compounds was evaluated by C, H, N analysis (Atlantic Microlabs). The purity of all the final compounds was confirmed to be \geq 95% by combustion.

General Procedure A. To a solution of chloral hydrate in water were added sodium sulfate (6 equiv) and appropriate aniline (1 equiv) followed by a solution of hydroxylamine hydrochloride solution (3 equiv) in water. The reaction mixture was heated at 55 °C with stirring overnight and then cooled to room temperature. The resulting precipitate was filtered and dried to obtain the isonitrosoacetanilide intermediates. The isonitrosoacetanilide was added to a stirring solution of concentrated sulfuric acid slowly to keep the temperature in the range of 60–70 °C. Upon completion of the addition, the

mixture was heated to 80 °C for 10 min and then poured into crushed ice and stirred for 30 min. The precipitate was filtered and washed three times with water and dried under vacuum to afford the solids 5a–e.

General Procedure B. To a solution of 4,7-dichloroisatin (1.0 equiv) were added appropriate acetophenone (4.0 equiv) and catalytic amount diethylamine (10 drops) in methanol. The mixture was stirred at room temperature until the starting material (4,7-dichloroisatin) disappeared completely. The resulted solution was concentrated and purified with flash chromatography, eluting with hexane/ethyl acetate to afford product in quantitative yield. The product was recrystallized with hexanes/ethyl acetate to give a pure product.

4-Chloroindoline-2,3-dione (5a). Compound 5a was prepared via general procedure A from 3a (500 mg, 3.88 mmol), chloral hydrate (965 mg, 5.83 mmol), hydroxylamine hydrochloride (808 mg, 11.6 mmol), sodium sulfate (3.42 g, 23.3 mmol), and 1 N HCl (8 mL) to yield a dark brown solid (580 mg, 82.3%). ¹H NMR (DMSO-*d*₆, 400 Hz) δ 11.17 (s, 1H), 7.53 (t, 1H, *J* = 16.4), 7.06 (d, 1H, *J* = 8), 6.87 (d, 1H, *J* = 8).

5-Chloroindoline-2,3-dione (5b). Compound 5b was prepared via general procedure A from 3b (500 mg, 3.88 mmol), chloral hydrate (965 mg, 5.83 mmol), hydroxylamine hydrochloride (808 mg, 11.64 mmol), sodium sulfate (3.42 g, 23.3 mmol), and 1 N HCl (8 mL) to yield a brown solid (600 mg, 85%). ¹H NMR (DMSO-*d*₆, 400 Hz) δ 11.24 (s, 1H), 7.62–7.59 (m, 1H), 7.535 (s, 1H), 6.92 (d, 1H, *J* = 8.4).

5,6-Dichloroindoline-2,3-dione (5c). Compound 5c was prepared via general procedure A from 3c (500 mg, 2.31 mmol), chloral hydrate (574 mg, 3.47 mmol), hydroxylamine hydrochloride (482 mg, 6.94 mmol), sodium sulfate (2.04 g, 13.9 mmol), and 1 N HCl (4 mL) to yield a brown solid (370 mg, 74%). ¹H NMR (DMSO-*d*₆, 400 Hz) δ 11.24 (s, 1H), 7.7 (d, 1H, *J* = 9.2), 6.86 (d, 1H, *J* = 8.4).

4,7-Difluoroindoline-2,3-dione (5d). Compound 5d was prepared via general procedure A from 3d (400 μ L, 3.96 mmol), chloral hydrate (722 mg, 4.36 mmol), hydroxylamine hydrochloride (827 mg, 11.9 mmol), sodium sulfate (3.49 g, 23.8 mmol), and 1 N HCl (8 mL) to yield an orange solid (507 mg, 70%). ¹H NMR (DMSO-*d*₆, 400 Hz) δ 11.704 (s, 1H), 7.60–7.55 (m, 1H), 6.88–6.23 (m, 1H). ¹⁹F NMR (DMSO-*d*₆, 367 Hz) δ –138.21.

4,7-Dimethoxyindoline-2,3-dione (5e). Compound 5e was prepared via general procedure A from 3e (400 mg, 2.61 mmol), chloral hydrate (433.2 mg, 2.61 mmol), hydroxylamine hydrochloride (548 mg, 7.83 mmol), sodium sulfate (2.3 g, 15.7 mmol), and 1 N HCl (5.5 mL) to yield a brown solid (184 mg, 34%). ¹H NMR (DMSO-*d*₆, 400 Hz) δ 11.70 (s, 1H), 7.32 (d, 1H, *J* = 9.2), 6.62 (d, 1H, *J* = 9.2), 3.80 (s, 3H), 3.78 (s, 3H).

4-Chloro-3-hydroxy-3-(2-(4-methoxyphenyl)-2-oxoethyl)-indolin-2-one (6a). Compound 6a was prepared via general procedure B from 5a (50 mg, 0.27 mmol) and 4-methoxyacetophenone (165.4 mg, 1.10 mmol) to yield a white solid (84 mg, 92%); mp 224–226 °C. ¹H NMR (DMSO-*d*₆, 400 Hz) δ 10.51 (s, 1H), 7.90 (d, 2H, *J* = 8.8), 7.22 (t, 1H, *J* = 16), 7.04 (d, 2H, *J* = 8.8), 6.86 (q, 2H), 6.25 (s, 1H), 4.37 (d, 1H, *J* = 18), 3.85 (s, 3H), 3.63 (d, 1H, *J* = 18). ¹³C NMR (DMSO-*d*₆, 100 Hz) δ 195.17, 177.98, 163.88, 145.65, 131.06, 130.66 (2C), 130.09, 129.18, 128.27, 122.41, 114.47 (2C), 108.97, 74.38, 56.03, 44.35. HRMS (ES) *m/z* calcd for C₁₇H₁₄ClNO₄ (M – H)⁺ 330.0533; found, 330.0524. Anal. Calcd for C₁₇H₁₄ClNO₄: C, 61.55; H, 4.25; N, 4.22. Found: C, 61.6; H, 4.34; N, 4.26.

5-Chloro-3-hydroxy-3-(2-(4-methoxyphenyl)-2-oxoethyl)-indolin-2-one (6b). Compound 6b was prepared via general procedure B from 5b (50 mg, 0.27 mmol) and 4-methoxyacetophenone (165 mg, 1.10 mmol) to yield a white solid (85 mg, 93.4%); mp 191 °C. ¹H NMR (DMSO-*d*₆, 400 Hz) δ 10.37 (s, 1H), 7.88 (d, 2H, *J* = 8.8), 7.38 (s, 1H), 7.23 (q, 1H), 7.04 (d, 2H, *J* = 8.8), 6.83 (d, 1H, *J* = 8.4), 6.16 (s, 1H), 4.11 (d, 1H, *J* = 17.6), 3.84 (s, 3H), 3.59 (d, 1H, *J* = 17.6). ¹³C NMR (DMSO-*d*₆, 100 Hz) δ 195.28, 178.57, 163.79, 142.38, 134.57, 130.75 (2C), 129.49, 129.02, 125.55, 124.35, 114.35 (2C), 111.21, 73.57, 56.04, 45.85. HRMS (ES) *m/z* calcd for C₁₇H₁₄ClNO₄ (M – H)⁺ 330.0533; found, 330.0529. Anal. Calcd for C₁₇H₁₄ClNO₄: C, 61.55; H, 4.25; N, 4.22. Found: C, 61.46; H, 4.55; N, 4.09.

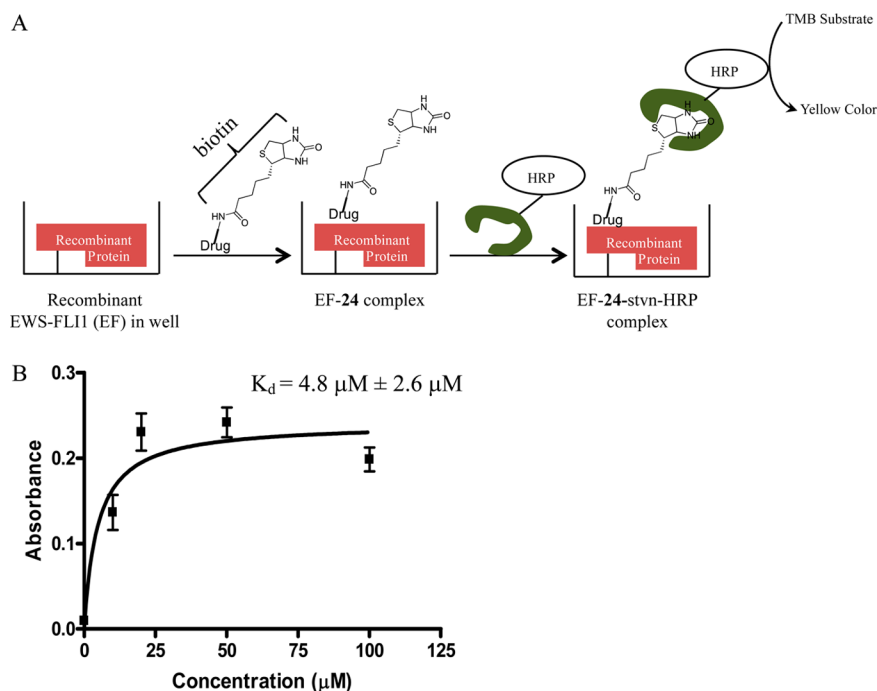


Figure 6. (A) Schematic overview of ELISA-like assay to probe the binding of the biotin conjugate to recombinant EWS-FLI1. (B) Saturation curve of biotin conjugate (**24**) to recombinant EWS-FLI1.

5,6-Dichloro-3-hydroxy-3-(2-(4-methoxyphenyl)-2-oxoethyl)indolin-2-one (6c). Compound **6c** was prepared via general procedure B from **5c** (50 mg, 0.23 mmol) and 4-methoxyacetophenone (139 mg, 0.92 mmol) to yield a white solid (79 mg, 95%); mp 214–215 °C. ^1H NMR (DMSO- d_6 , 400 Hz) δ 10.64 (s, 1H), 7.91 (d, 2H, J = 8.4), 7.47 (d, 1H, J = 8.4), 7.04 (d, 2H, J = 9.2), 6.85 (d, 1H, J = 8.4), 6.38 (s, 1H), 4.37 (d, 1H, J = 18), 3.85 (s, 3H), 3.68 (d, 1H, J = 18). ^{13}C NMR (DMSO- d_6 , 100 Hz) δ 195.18, 177.79, 163.97, 144.21, 131.17, 130.77, 130.73 (2C), 130.50, 129.01, 114.50 (2C), 110.15, 75.03, 73.24, 56.05, 44.34. Anal. Calcd for $\text{C}_{17}\text{H}_{13}\text{Cl}_2\text{NO}_4$: C, 55.76; H, 3.58; N, 3.82. Found: C, 55.82; H, 3.60; N, 3.88.

4,7-Difluoro-3-hydroxy-3-(2-(4-methoxyphenyl)-2-oxoethyl)indolin-2-one (6d). Compound **6d** was prepared via general procedure B from **5d** (50 mg, 0.27 mmol) and 4-methoxyacetophenone (164 mg, 1.09 mmol) to yield a light pink solid (83.6 mg, 93%); mp 170 °C. ^1H NMR (DMSO- d_6 , 400 Hz) δ 10.96 (s, 1H), 7.87 (d, 2H, J = 8.8), 7.17–7.11 (m, 1H), 7.01 (d, 2H, J = 9.2), 6.8–6.62 (m, 1H), 6.45 (s, 1H), 4.03 (d, 1H, J = 17.6), 3.82 (s, 3H), 3.66 (d, 1H, J = 18). ^{13}C NMR (DMSO- d_6 , 100 Hz) δ 195.18, 177.82, 163.99, 149.24, 130.76, 129.09 (2C), 119.78, 118.11, 114.49, 109.47 (2C), 109.23, 104.99, 73.48, 56.06, 45.17. ^{19}F NMR (DMSO- d_6 , 367 Hz) δ -138.62. HRMS (ES) m/z calcd for $\text{C}_{17}\text{H}_{13}\text{F}_2\text{NO}_4$ ($M - \text{H}$) $^+$ 332.0734; found, 332.0735. Anal. Calcd for $\text{C}_{17}\text{H}_{13}\text{F}_2\text{NO}_4$: C, 61.26; H, 3.93; N, 4.20. Found: 61.45; H, 3.93; N, 4.30.

3-Hydroxy-4,7-dimethoxy-3-(2-(4-methoxyphenyl)-2-oxoethyl)indolin-2-one (6e). Compound **6e** was prepared via general procedure B from **5e** (50 mg, 0.24 mmol) and 4-methoxyacetophenone (144 mg, 0.96 mmol) to yield a brown solid (31.4 mg, 35%). ^1H NMR (DMSO- d_6 , 400 Hz) δ 10.16 (s, 1H), 7.82 (d, 2H, J = 9.2), 6.99 (d, 2H, J = 9.2), 6.81 (d, 1H, J = 9.2), 6.39 (d, 2H, J = 8.8), 5.85 (s, 1H), 4.17 (d, 1H, J = 16.8), 3.80 (s, 3H), 3.73 (s, 3H), 3.59 (s, 3H), 3.41 (d, 1H, J = 16.8). Anal. Calcd for $\text{C}_{19}\text{H}_{19}\text{NO}_6$: C, 63.86; H, 5.36; N, 3.92. Found: C, 63.78; H, 5.69; N, 3.90.

3-Hydroxy-3-(2-(4-methoxyphenyl)-2-oxoethyl)-4,7-dimethylindolin-2-one (6f). Compound **6f** was prepared via general procedure B from **5f** (50 mg, 0.28 mmol) and 4-methoxyacetophenone (172 mg, 1.14 mmol) to yield a brown solid (87.4 mg, 96%); mp 135–136 °C. ^1H NMR (DMSO- d_6 , 400 Hz) δ 10.18 (s, 1H), 7.86 (d, 2H, J = 9.2), 6.99 (d, 2H, J = 8.8), 6.84 (d, 1H, J = 7.6), 6.52 (d, 1H, J

= 7.6), 5.91 (s, 1H), 4.04 (d, 1H, J = 17.2), 3.80 (s, 3H), 3.54 (d, 1H, J = 17.2), 2.20 (s, 3H), 2.13 (s, 3H). ^{13}C NMR (DMSO- d_6 , 100 Hz) δ 195.085, 179.15, 163.72, 141.92, 132.01 (2C), 130.68, 130.43, 129.55, 128.73, 123.84, 116.36, 114.37 (2C), 74.70, 56.00, 45.03, 17.42, 16.57. Anal. Calcd for $\text{C}_{19}\text{H}_{19}\text{NO}_4 \cdot \frac{1}{4}\text{EtOAc}$: C, 69.15; H, 6.09; N, 4.03. Found: C, 69.10; H, 6.04; N, 4.15.

7-Chloro-3-hydroxy-3-(2-(4-methoxyphenyl)-2-oxoethyl)indolin-2-one (6g). Compound **6g** was prepared via procedure B from commercially available 7-chloroisatin (50 mg, 0.27 mmol) and 4-methoxyacetophenone (165.4 mg, 1.10 mmol) to yield a white solid (84 mg, 92%). ^1H NMR (DMSO- d_6 , 400 Hz) δ 10.66 (s, 1H), 7.87 (d, 2H, J = 8.8), 7.25 (dd, 2H, J = 12.4), 7.02 (d, 2H, J = 8.8), 6.90 (t, 1H, J = 15.6), 6.18 (s, 1H), 4.06 (d, 1H, J = 18), 3.83 (s, 3H), 3.60 (d, 1H, J = 18). ^{13}C NMR (DMSO- d_6 , 100 Hz) δ 195.25, 178.75, 163.82, 141.17, 134.44, 130.85 (2C), 129.43, 129.29, 122.94, 122.53, 114.28, 114.05, 74.03, 56.04, 46.04. HRMS (ES) m/z calcd for $\text{C}_{17}\text{H}_{14}\text{ClNO}_4$ ($M - \text{H}$) $^+$ 330.0533; found, 330.0330. Anal. Calcd for $\text{C}_{17}\text{H}_{14}\text{ClNO}_4 \cdot 0.1\text{EtOAc}$: C, 61.37; H, 4.38; N, 4.11. Found: C, 61.27; H, 4.48; N, 4.19.

3-Hydroxy-3-(2-(4-methoxyphenyl)-2-oxoethyl)indolin-2-one (6h). Compound **6h** was prepared via general procedure B from commercially available isatin (50 mg, 0.34 mmol) and 4-methoxyacetophenone (204.1 mg, 1.56 mmol) to yield a white solid (75 mg, 79.01%); mp 187 °C. ^1H NMR (DMSO- d_6 , 400 Hz) δ 10.20 (s, 1H), 7.85 (d, 2H, J = 9.2), 7.24 (d, 1H, J = 7.2), 7.15 (d, 1H, J = 15.6), 6.99 (d, 2H, J = 8.8), 6.84–6.77 (m, 2H, J = 7.6, 7.6), 5.99 (s, 1H), 3.99 (d, 1H, J = 17.2), 3.80 (s, 3H), 3.51 (d, 1H, J = 17.2). ^{13}C NMR (DMSO- d_6 , 100 Hz) δ 195.17, 178.83, 163.67, 143.4, 132.31, 130.68 (2C), 129.66, 129.28, 123.97, 121.49, 114.3 (2C), 109.19, 73.50, 55.98, 45.84. HRMS (ES) m/z calcd for $\text{C}_{17}\text{H}_{15}\text{NO}_4$ ($M + \text{H}$) $^+$ 298.1079; found, 298.1076. Anal. Calcd for $\text{C}_{17}\text{H}_{15}\text{NO}_4$: C, 68.68; H, 5.09; N, 4.71. Found: C, 68.42; H, 5.25; N, 4.71.

4,7-Dichloro-3-hydroxy-3-(2-(2-methoxyphenyl)-2-oxoethyl)indolin-2-one (9a). Compound **9a** was prepared via general procedure B from 4,7-dichloroisatin (100 mg, 0.46 mmol) and **8a** (256 μL , 1.84 mmol) to yield a white solid (150 mg, 89.05%); mp 183–184 °C. ^1H NMR (DMSO- d_6 , 400 Hz) δ 10.91 (s, 1H), 7.53 (t, 1H, J = 8.8), 7.35 (d, 1H, J = 8.8), 7.27 (d, 1H, J = 8.8), 7.16 (d, 1H, J = 8.4), 6.94 (t, 1H, J = 7.6), 6.86 (d, 1H, J = 8.8), 6.34 (s, 1H), 4.33 (d, 1H, J = 18.4), 3.90 (s, 3H), 3.66 (d, 1H, J = 18.4). ^{13}C NMR (DMSO-

d_6 , 100 Hz) δ 197.7, 177.9, 159.2, 143.03, 135.00, 130.76, 129.84, 129.81, 128.64, 126.47, 123.58, 120.92, 113.19, 113.06, 74.92, 56.36, 50.04. HRMS (ES) m/z calcd for $C_{17}H_{13}Cl_2NO_4$ ($M - H$)⁺ 364.0143; found, 364.0142. Anal. Calcd for $C_{17}H_{13}Cl_2NO_4$: C, 55.76; H, 3.58; N, 3.82. Found: C, 55.57; H, 3.52; N, 3.83;

4,7-Dichloro-3-hydroxy-3-(2-(3-methoxyphenyl)-2-oxoethyl)indolin-2-one (9b). Compound **9b** was prepared via general procedure B from 4,7-dichloroisatin (100 mg, 0.46 mmol) and **8b** (253 μ L, 1.84 mmol) to yield a light pink solid (163 mg, 96.7%); mp 154–155 °C. ¹H NMR (DMSO- d_6 , 400 MHz) δ 10.97 (s, 1H), 7.53 (d, 1H, $J = 7.6$), 7.42 (t, 1H, $J = 28$), 7.31 (s, 1H), 7.28 (d, 1H, $J = 8.4$), 7.19 (d, 1H, $J = 10$), 6.88 (d, 1H, $J = 8.8$), 6.43 (s, 1H), 4.34 (d, 1H, $J = 18.4$), 3.75 (s, 3H), 3.71 (d, 1H, $J = 18.4$). ¹³C NMR (DMSO- d_6 , 100 Hz) δ 196.75, 177.8, 159.89, 143.06, 137.25, 130.88, 130.52, 129.7, 128.66, 123.64, 120.99, 120.58, 113.29, 112.3, 74.99, 55.75, 44.9. HRMS (ES) m/z calcd for $C_{17}H_{13}Cl_2NO_4$ ($M - H$)⁺ 364.0143; found, 364.0142. Anal. Calcd for $C_{17}H_{13}Cl_2NO_4 \cdot 1/4 EtOAc$: C, 55.69; H, 3.89; N, 3.61. Found: C, 55.45; H, 3.56, N, 3.82.

4,7-Dichloro-3-(2-(2,4-dimethoxyphenyl)-2-oxoethyl)-3-hydroxyindolin-2-one (9c). Compound **9c** was prepared via general procedure B from 4,7-dichloroisatin (100 mg, 0.46 mmol) and **8c** (332 mg, 1.84 mmol) to yield a white solid (142 mg, 78.3%); mp 195–196 °C. ¹H NMR (DMSO- d_6 , 400 Hz) δ 10.86 (s, 1H), 7.46 (d, 1H, $J = 8.8$), 7.26 (d, 1H, $J = 8.8$), 6.85 (d, 1H, $J = 8.8$), 6.628 (s, 1H), (6.52 (dd, 1H, $J = 10.8$), 6.28 (s, 1H), 4.29 (d, 1H, $J = 18.8$), 3.92 (s, 3H), 3.79 (s, 3H), 3.62 (d, 1H, $J = 18.8$). ¹³C NMR (DMSO- d_6 , 100 Hz) δ 196.01, 178.88, 166.01, 162.39, 143.91, 132.98, 131.42, 130.98, 129.28, 124.31, 119.95, 113.94, 107.50, 99.69, 75.80, 57.27, 56.92, 50.78. HRMS (ESI) m/z calcd for $C_{18}H_{15}Cl_2NO_5$ ($M + H$)⁺ 396.0406; found, 396.0389. Anal. Calcd for $C_{18}H_{15}Cl_2NO_5 \cdot EtOAc$: C, 54.56; H, 4.79; N, 2.89. Found: C, 53.51; H 4.02; N 3.42.

4,7-Dichloro-3-(2-(3,5-dimethoxyphenyl)-2-oxoethyl)-3-hydroxyindolin-2-one (9d). Compound **9d** was prepared via general procedure B from 4,7-dichloroisatin (100 mg, 0.46 mmol) and **8d** (332 mg, 1.84 mmol) to yield a white solid (112 mg, 67.2%); mp 204–205 °C. ¹H NMR (DMSO- d_6 , 400 Hz) δ 10.96 (s, 1H), 7.28 (d, 1H, $J = 8.4$), 6.99 (s, 2H), 6.88 (d, 1H, $J = 8.8$), 6.73 (s, 1H), 6.41 (s, 1H), 4.34 (d, 1H, $J = 18.4$), 3.75 (s, 6H), 3.71 (s, 1H, $J = 18.4$). ¹³C NMR (DMSO- d_6 , 100 Hz) δ 196.59, 177.78, 161.06 (2C), 143.06, 137.86, 130.87, 129.72, 128.67, 123.65, 113.29, 106.32, 105.93 (2C), 75.02, 55.96 (2C), 44.96. HRMS (ES) m/z calcd for $C_{18}H_{15}Cl_2NO_5$ ($M - H$)⁺ 394.0249; found, 394.0251. Anal. Calcd for $C_{18}H_{15}Cl_2NO_5$: C, 54.56; H, 3.82; N, 3.54. Found: C, 54.76; H, 3.91; N, 3.56.

4,7-Dichloro-3-(2-(2,3-dimethoxyphenyl)-2-oxoethyl)-3-hydroxyindolin-2-one (9e). Compound **9e** was prepared via general procedure B from 4,7-dichloroisatin (100 mg, 0.46 mmol) and **8e** (230 mg, 1.27 mmol) to yield a white solid (132.2 mg, 72.6%); mp 203–204 °C. ¹H NMR (DMSO- d_6 , 400 Hz) δ 10.96 (s, 1H), 7.28 (d, 1H, $J = 8.8$), 7.24 (d, 1H, $J = 8$), 7.07 (t, 1H, $J = 16$), 6.89 (t, 2H, $J = 8.4$), 6.40 (s, 1H), 4.33 (d, 1H, $J = 18.8$), 3.8 (s, 6H), 3.67 (s, 1H, $J = 18.8$). ¹³C NMR (DMSO- d_6 , 100 Hz) δ 198.32, 177.87, 135.24, 148.57, 143.06, 131.87, 130.86, 129.64, 128.7, 124.57, 123.63, 120.31, 117.48, 113.26, 74.83, 61.42, 59.47, 49.40. HRMS (ES) m/z calcd for $C_{18}H_{15}Cl_2NO_5$ ($M - H$)⁺ 394.0249; found, 394.0254. Anal. Calcd for $C_{18}H_{15}Cl_2NO_5$: C, 54.56; H, 3.82; N, 3.54. Found: C, 54.29; H, 3.75; N, 3.53.

4,7-Dichloro-3-hydroxy-3-(2-oxo-2-(2,3,4-trimethoxyphenyl)ethyl)indolin-2-one (9f). Compound **9f** was prepared via general procedure B from 4,7-dichloroisatin (100 mg, 0.46 mmol) and **8f** (336 μ L, 1.84 mmol) to yield a white solid (163.5 mg, 83.4%); mp 162–163 °C. ¹H NMR (DMSO- d_6 , 400 Hz) δ 10.91 (s, 1H), 7.27 (q, 2H), 6.87 (q, 2H), 6.36 (s, 1H), 4.33 (d, 1H, $J = 18.4$), 3.88 (s, 3H), 3.81 (s, 3H), 3.73 (s, 3H), 3.67 (s, 1H, $J = 18.4$). ¹³C NMR (DMSO- d_6 , 100 Hz) δ 195.89, 177.97, 158.10, 154.17, 143.09, 142.0, 130.73, 129.93, 128.58, 125.37, 123.99, 123.56, 113.2, 108.34, 74.92, 61.82, 60.87, 56.57, 49.06. HRMS (ESI) m/z calcd for $C_{19}H_{17}Cl_2NO_6$ ($M + H$)⁺ 426.0511; found, 426.0504. Anal. Calcd for $C_{19}H_{17}Cl_2NO_6$: C, 53.54; H, 4.02; N, 3.29. Found: C, 53.50, H 4.00, N 3.21.

4,7-Dichloro-3-hydroxy-3-(2-oxo-2-phenylethyl)-1,3-dihydroindol-2-one (9g). Compound **9g** was prepared via general procedure B from 4,7-dichloroisatin (100 mg, 0.46 mmol) and **8g** (253 μ L, 1.84 mmol) to yield a white solid (163 mg, 96.7%); mp 198–200 °C. ¹H NMR (DMSO- d_6 , 400 MHz) δ 10.97 (s, 1H), 7.88 (dd, 2H, $J = 0.8, 1.6$ Hz), 7.62 (m, 1H), 7.48 (t, 2H, $J = 8.4, 7.2$ Hz), 7.27 (d, 1H, $J = 8.8$ Hz), 6.87 (d, 1H, $J = 8.8$ Hz), 6.43 (s, 1H), 4.36 (d, 1H, $J = 18.4$ Hz), 3.68 (d, 1H, $J = 18.4$ Hz). Anal. Calcd for $C_{16}H_{11}Cl_2NO_3$: C, 57.17; H, 3.30; N, 4.17. Found: C, 56.99, H, 3.81, N, 3.75.

4,7-Dichloro-3-[2-(4-fluorophenyl)-2-oxoethyl]-3-hydroxy-1,3-dihydroindol-2-one (9h). Compound **9h** was prepared via general procedure B from 4,7-dichloroisatin (100 mg, 0.46 mmol) and **8h** (256 mg, 1.84 mmol) to yield light a yellow solid (140 mg, 85.9%); mp 176–178 °C. ¹H NMR (DMSO- d_6 , 400 MHz) δ 10.98 (s, 1H), 7.98 (m, 2H), 7.29 (m, 3H), 6.87 (d, 1H, $J = 8.4$ Hz), 6.43 (s, 1H), 4.34 (d, 1H, $J = 18.4$ Hz), 3.68 (d, 1H, $J = 18.4$ Hz). Anal. Calcd for $C_{16}H_{10}Cl_2FNO_3$: C, 54.26; H, 2.85; N, 3.95. Found: C, 54.58, H, 3.50, N, 3.53.

4,7-Dichloro-3-hydroxy-3-[2-(4-iodophenyl)-2-oxoethyl]-1,3-dihydroindol-2-one (9i). Compound **9i** was prepared via general procedure B from 4,7-dichloroisatin (100 mg, 0.46 mmol) and **8i** (455.2 mg, 1.84 mmol) to yield a light yellow solid (230 mg, 100%); mp 190–192 °C. ¹H NMR (DMSO- d_6 , 400 MHz) δ 10.98 (s, 1H), 7.87 (d, 2H, $J = 8.8$ Hz), 7.64 (d, 2H, $J = 8.8$ Hz), 7.27 (d, 1H, $J = 8.8$ Hz), 6.87 (d, 1H, $J = 8.8$ Hz), 6.44 (s, 1H), 4.30 (d, 1H, $J = 18.4$ Hz), 3.65 (d, 1H, $J = 18.4$ Hz). Anal. Calcd for $C_{16}H_{10}Cl_2INO_3$ ·EtOAc: C, 43.62; H, 3.27; N, 2.78. Found: C, 43.96, H, 2.88, N, 2.88.

4,7-Dichloro-3-hydroxy-3-(2-oxo-2-(4-(trifluoromethyl)phenyl)ethyl)indolin-2-one (9j). Compound **9j** was prepared via general procedure B from 4,7-dichloroisatin (100 mg, 0.46 mmol) and **8j** (346.2 mg, 1.84 mmol) to yield a white solid (165 mg, 86.8%); mp 176.5–178 °C. ¹H NMR (DMSO- d_6 , 400 Hz) δ 11.01 (s, 1H), 8.09 (d, 2H, $J = 7.6$), 7.86 (d, 2H, $J = 8.4$), 7.291 (d, 1H, $J = 8.8$), 6.88 (d, 1H, $J = 8.8$), 6.49 (d, 1H), 4.40 (d, 1H, $J = 18$), 3.76 (d, 1H, $J = 18$). ¹³C NMR (DMSO- d_6 , 100 Hz) δ 196.6, 177.68, 143.03, 138.97, 131.04, 129.46, 129.27 (3C), 128.76, 126.34, 126.31, 123.4 (2C), 113.4, 74.9, 45.07. HRMS (ES) m/z calcd for $C_{17}H_{10}Cl_2F_3NO_3$ ($M - H$)⁺ 401.9912; found, 401.991. Anal. Calcd for $C_{17}H_{10}Cl_2F_3NO_3$: C, 50.52; H, 2.49; N, 3.47. Found: C, 49.88; H, 2.6; N, 3.44.

4-(2-(4,7-Dichloro-3-hydroxy-2-oxoindolin-3-yl)acetyl)benzotrile (9k). Compound **9k** was prepared via general procedure B from 4,7-dichloroisatin (100 mg, 0.46 mmol) and **8k** (455.2 mg, 1.84 mmol) to yield a white solid (93 mg, 64%); mp 195–196 °C. ¹H NMR (DMSO- d_6 , 400 Hz) δ 11.01 (s, 1H), 8.06 (d, 2H, $J = 10$), 7.97 (d, 2H, $J = 10.5$), 7.30 (d, 1H, $J = 15$), 6.89 (d, 1H, $J = 11$), 6.49 (s, 1H), 4.39 (d, 1H, $J = 23$), 3.79 (d, 1H, $J = 23$). ¹³C NMR (DMSO- d_6 , 100 Hz) δ 196.57, 177.61, 142.94, 138.88, 133.37 (2C), 131.03, 129.39, 129.03 (2C), 128.73, 123.72, 118.47, 116.17, 113.36, 74.94, 45.05. HRMS (ES) m/z calcd for $C_{17}H_{10}Cl_2N_2O_3$ ($M - H$)⁺ 358.9990; found, 358.9990. Anal. Calcd for $C_{17}H_{10}Cl_2N_2O_3$: C, 56.53; H, 2.79; N, 7.76. Found: C, 56.29; H, 2.77; N, 7.6.

4,7-Dichloro-3-hydroxy-3-(2-oxo-2-*p*-tolylethyl)-1,3-dihydroindol-2-one (9m). Compound **9m** was prepared via general procedure B from 4,7-dichloroisatin (100 mg, 0.46 mmol) and **8m** (248.2 mg, 1.84 mmol) to yield a light yellow solid (152 mg, 100%); mp 189–192 °C. ¹H NMR (DMSO- d_6 , 400 MHz) δ 10.95 (s, 1H), 7.78 (d, 2H, $J = 8.4$ Hz), 7.27 (m, 3H), 6.86 (d, 1H, $J = 8.8$ Hz), 6.41 (s, 1H), 4.33 (d, 1H, $J = 18.4$ Hz), 3.64 (d, 1H, $J = 18.4$ Hz), 2.33 (s, 3H). Anal. Calcd for $C_{17}H_{13}Cl_2NO_3 \cdot 1/2 EtOAc$: C, 57.82; H, 4.31; N, 3.55. Found: C, 57.60, H, 4.23, N, 3.56.

4,7-Dichloro-3-(2-(4-ethoxyphenyl)-2-oxoethyl)-3-hydroxyindolin-2-one (9n). Compound **9n** was prepared via general procedure B from 4,7-dichloroisatin (100 mg, 0.46 mmol) and **8n** (302.2 mg, 1.84 mmol) to yield a white solid (164 mg, 93.8%); mp 162–163 °C. ¹H NMR (400 Hz, DMSO- d_6) δ 10.93 (s, 1H), 7.86 (d, 2H, $J = 9.2$), 7.28 (d, 1H, $J = 8.8$), 6.99 (d, 2H, $J = 9.2$), 6.88 (d, 1H, $J = 8.8$), 6.38 (s, 1H), 4.34 (d, 1H, $J = 18$), 4.12 (q, 2H), 3.64 (d, 1H, $J = 18$), 1.34 (t, 3H, $J = 14$). ¹³C NMR (100 Hz, DMSO- d_6): 194.7, 177.5, 162.8, 142.7, 130.4 (2C), 130.3, 129.4, 128.3, 128.2, 123.1, 114.4 (2C), 112.7, 74.6, 63.6, 43.9, 14.45. HRMS (ES) m/z calcd for

$C_{18}H_{15}Cl_2NO_4$ ($M - H$)⁺ 378.0300; found, 378.0307. Anal. Calcd for $C_{18}H_{15}Cl_2NO_4 \cdot 3.5EtOAc$: C, 56.69; H, 4.36; N, 3.41. Found: C, 56.38; H, 4.08; N, 3.56.

4,7-Dichloro-3-hydroxy-3-(2-(4-isopropoxyphenyl)-2-oxoethyl)indolin-2-one (9p). Compound **9p** was prepared via general procedure B from 4,7-dichloroisatin (100 mg, 0.46 mmol) and **8p** (327.5 mg, 1.84 mmol) to yield a white solid (152.2 mg, 83.9%); mp 168–169 °C. ¹H NMR (DMSO-*d*₆, 400 Hz) δ 10.93 (s, 1H), 7.84 (d, 2H, *J* = 8.8), 7.28 (d, 1H, *J* = 8.8), 6.97 (d, 2H, *J* = 8.8), 6.88 (d, 1H, *J* = 8.8), 6.38 (s, 1H), 4.74–4.68 (m, 1H), 4.33 (d, 1H, *J* = 18), 3.64 (d, 1H, *J* = 18), 1.263 (s, 3H), 1.248 (s, 3H). ¹³C NMR (DMSO-*d*₆, 100 Hz): 195.13, 177.92, 162.39, 143.13, 130.83 (2C), 130.8, 129.9, 128.65, 128.55, 123.61, 115.66 (2C), 113.26, 104.9, 75.09, 70.24, 44.41, 22.14. HRMS (ESI) *m/z* calcd for $C_{19}H_{17}Cl_2NO_4$ ($M + H$)⁺ 394.0613; found, 394.0602. Anal. Calcd for $C_{20}H_{19}Cl_2NO_4 \cdot 1/2EtOAc$: C, 58.38; H, 5.16; N, 3.07. Found: C, 57.79; H, 4.59; N, 3.48.

4,7-Dichloro-3-hydroxy-3-(2-oxo-2-(4-phenoxyphenyl)ethyl)indolin-2-one (9q). Compound **9q** was prepared via general procedure B from 4,7-dichloroisatin (100 mg, 0.46 mmol) and **8q** (390.5 mg, 1.84 mmol) to yield a white solid (137 mg, 82.9%); mp 169–170 °C. ¹H NMR (DMSO-*d*₆, 400 Hz) δ 10.95 (s, 1H), 7.93 (d, 2H, *J* = 8.4), 7.46 (t, 2H, *J* = 15.2), 7.28 (d, 1H, *J* = 8), 7.26 (d, 1H, *J* = 8), 7.23 (d, 1H, *J* = 8), 7.12 (d, 1H, *J* = 8), 6.99 (d, 2H, *J* = 8.4), 6.89 (d, 1H, *J* = 8.4), 6.41 (s, 1H), 4.34 (d, 1H, *J* = 18), 3.66 (d, 1H, *J* = 18). ¹³C NMR (DMSO-*d*₆, 100 Hz) δ 195.40, 177.84, 162.23, 155.19, 143.09, 140, 130.85, 130.8 (2C), 130.68, 129.78, 128.65, 125.37, 123.61, 120.62 (2C), 117.55 (2C), 113.28, 75.05, 44.58. HRMS (ESI) *m/z* calcd for $C_{22}H_{15}Cl_2NO_4$ ($M - H$)⁺ 426.0300; found, 426.0306. Anal. Calcd for $C_{22}H_{15}Cl_2NO_4$: C, 61.70; H, 3.53; N, 3.27. Found: C, 61.96; H, 3.56; N, 3.37.

4,7-Dichloro-3-hydroxy-3-(2-(4-(methylthio)phenyl)-2-oxoethyl)indolin-2-one (9r). Compound **9r** was prepared via general procedure B from 4,7-dichloroisatin (100 mg, 0.46 mmol) and **8r** (307.5 mg, 1.84 mmol) to yield a light yellow solid (152 mg, 86.4%); mp 182–182 °C. ¹H NMR (DMSO-*d*₆, 400 Hz) δ 10.96 (s, 1H), 7.82 (d, 2H, *J* = 7.6), 7.32 (d, 2H, *J* = 7.6), 7.284 (d, 1H, *J* = 10), 6.88 (d, 1H, *J* = 10), 6.43 (s, 1H), 4.36 (d, 1H, *J* = 18), 3.68 (d, 1H, *J* = 18). ¹³C NMR (DMSO-*d*₆, 100 Hz) δ 195.83, 177.84, 146.8, 143.08, 132.07, 130.86, 129.75 (2C), 128.81 (2C), 128.65, 125.34, 123.62, 113.28, 75.04, 44.53, 14.31. HRMS (ESI) *m/z* calcd for $C_{17}H_{13}Cl_2NO_3S$ ($M + H$)⁺ 382.0071; found, 382.0059. Anal. Calcd for $C_{17}H_{13}Cl_2NO_3S$: C, 53.41; H, 3.43; N, 3.66. Found: C, 53.63; H, 3.46; N, 3.74.

3-[2-(4-Aminophenyl-2-oxoethyl)]-4,7-dichloro-3-hydroxyl 1,3-dihydroindol-2-one (9s). Compound **9s** was prepared via general procedure B from 4,7-dichloroisatin (90 mg, 0.43 mmol) and **8s** (116 mg, 0.86 mmol) to yield a white solid; mp 240–243 °C. ¹H NMR (DMSO-*d*₆, 400 MHz) δ 10.85 (s, 1H), 7.56 (d, 2H, *J* = 8.8 Hz), 7.24 (d, 1H, *J* = 8.8 Hz), 6.84 (d, 1H, *J* = 8.8 Hz), 6.49 (d, 2H, *J* = 8.8 Hz), 6.28 (s, 1H), 6.10 (s, 2H), 4.20 (d, 1H, *J* = 18.0 Hz), 3.45 (d, 1H, *J* = 17.6 Hz). Anal. Calcd for $C_{16}H_{12}Cl_2N_2O_3$: C, 54.72; H, 3.44; N, 7.98. Found: C, 54.71; H, 3.44; N, 7.76.

4,7-Dichloro-3-hydroxy-3-(2-(4-(methylamino)phenyl)-2-oxoethyl)indolin-2-one (9t). Compound **9t** was prepared via general procedure B from 4,7-dichloroisatin (100 mg, 0.46 mmol) and **8t** (274.5 mg, 1.84 mmol) to yield a white solid (154 mg, 91.4%); mp 214–215 °C. ¹H NMR (DMSO-*d*₆, 400 Hz) δ 10.86 (s, 1H), 7.67 (d, 2H, *J* = 8.8), 7.27 (d, 1H, *J* = 8.8), 6.88 (d, 1H, *J* = 8.8), 6.69 (d, 1H, *J* = 8.8), 6.53 (d, 2H, *J* = 7.6), 6.31 (s, 1H), 4.27 (d, 1H, *J* = 17.6), 3.52 (d, 1H, *J* = 17.6), 2.72 (s, 3H). ¹³C NMR (DMSO-*d*₆, 100 Hz) δ 193.66, 178.10, 154.59, 143.18, 130.67 (2C), 130.25, 128.61, 123.68, 123.51, 113.16, 75.27, 60.23, 43.95, 29.57, 21.25, 14.58. HRMS (ESI) *m/z* calcd for $C_{17}H_{14}Cl_2N_2O_3$ ($M + H$)⁺ 365.0381; found, 365.0440. Anal. Calcd for $C_{17}H_{14}Cl_2N_2O_3$: C, 55.91; H, 3.86; N, 7.67. Found: C, 55.88; H, 3.98; N, 7.51.

4,7-Dichloro-3-(2-(4-(dimethylamino)phenyl)-2-oxoethyl)-3-hydroxyindolin-2-one (9u). Compound **9u** was prepared via general procedure B from 4,7-dichloroisatin (100 mg, 0.46 mmol) and **8u** (300 mg, 1.84 mmol) to yield a white solid (142 mg, 81.4%); mp 205–207. ¹H NMR (DMSO-*d*₆, 400 Hz) δ 10.95 (s, 1H), 7.79 (d,

2H, *J* = 8), 7.29 (t, 3H, *J* = 6.8), 6.88 (d, 1H, *J* = 8.8), 6.412 (s, 1H), 4.37 (d, 1H, *J* = 18), 3.68 (d, 1H, *J* = 18), 2.34 (s, 6H). ¹³C NMR (DMSO-*d*₆, 100 Hz) δ 196.44, 177.84, 144.72, 143.08, 133.5, 130.85, 129.85 (2C), 129.76, 128.64, 128.43 (2C), 123.61, 113.26, 75.01, 44.64, 21.61 (2C). HRMS (ES) *m/z* calcd for $C_{18}H_{16}Cl_2N_2O_3$ ($M + H$)⁺ 379.0381; found, 379.0607. Anal. Calcd for $C_{18}H_{16}Cl_2N_2O_3$: C, 57.01; H, 4.25; N, 7.39. Found: C, 57.21; H, 4.80; N, 6.72.

(Z)-4,7-Dichloro-3-(2-(4-methoxyphenyl)-2-oxoethylidene)indolin-2-one (10). A solution of **2** (100 mg, 0.27 mmol) in 96% sulfuric acid (5 mL) was stirred at room temperature for 5 min and was then quenched with ice and extracted with $CHCl_3$ (3 × 25–50 mL). The combined organic layers were washed with brine, dried over Na_2SO_4 , and concentrated under pressure. The dried organic mixture was purified with flash chromatography, eluting with hexane/ethyl acetate to afford a yellow solid (54.9 mg, 58%); mp 253–254 °C. ¹H NMR (DMSO-*d*₆, 400 Hz) δ 11.3 (s, 1H), 7.97 (s, 1H), 7.88 (d, 2H, *J* = 8.8), 7.41 (d, 1H, *J* = 8.4), 7.11 (d, 1H, *J* = 11), 7.04 (d, 2H, *J* = 8.8), 3.83 (s, 3H). ¹³C NMR (100 Hz, DMSO-*d*₆): 193.15, 165.9, 164.1, 142.3, 138.5, 131.5 (2C), 131.4, 130.4, 129.0, 128.2, 124.2, 119.7, 114.5 (2C), 113.7, 56.1. HRMS (ES) *m/z* calcd for $C_{17}H_{11}Cl_2NO_3$ ($M + H$)⁺ 349.0194; found, 349.0170. Anal. Calcd for $C_{17}H_{11}Cl_2NO_3$: C, 58.64; H, 3.18; N, 4.02. Found: C, 58.35; H, 3.06; N, 4.11.

Crystal data for **10**, $C_{17}H_{11}Cl_2NO_3$: *M* = 348.17 g/mol, yellow, prism, $0.65 \times 0.56 \times 0.49$ mm³, monoclinic, $P2_1/c$ (No. 14), *a* = 8.9990 (3) Å, *b* = 15.8170 (5) Å, *c* = 11.6532 (4) Å, β = 111.787° (1°), *V* = 1540.20 (9) Å³ (from 9955 reflections, θ = 2.3–29.7°), *Z* = 4, *D*_c = 1.501 g/cm³, *F*₀₀₀ = 712, Bruker APEXII CCD, Mo *K*α radiation, λ = 0.710 73 Å, *T* = 223(2) K, $2\theta_{max}$ = 56.0°, 14 380 reflections collected, 3711 unique (*R*_{int} = 0.0186). Final GOF = 1.043, *R*₁ = 0.0351, *wR*₂ = 0.0953, *R* indices based on 3313 reflections with *I* > 2σ(*I*) (refinement on *F*²), 252 parameters, 0 restraints, (Δ / σ)_{max} < 0.001, $\Delta\rho_{max}$ = 0.41 e Å⁻³, $\Delta\rho_{min}$ = -0.57 e Å⁻³. Lp and absorption corrections applied, μ = 0.44 mm⁻¹.

4,7-Dichloro-3-methoxy-3-(2-(4-methoxyphenyl)-2-oxoethyl)indolin-2-one (11). To a solution of **2** (75 mg, 0.20 mmol) in THF (5 mL) was added Mel (50 μL) at rt. The mixture was treated with 1.6 mmol of Ag₂O. The progress of reaction was monitored by TLC (12 h). When complete, the reaction mixture was filtered over Celite. The filtrate was washed with saturated solutions of sodium sulfite, sodium bicarbonate, and brine, dried and evaporated. The residue was purified on silica gel column using hexane/EtOAc (9:1) as an eluent to afford an oil **11** (44.8 mg, 58%). ¹H NMR (CDCl₃, 400 Hz) δ 7.86 (d, 2H, *J* = 8.8), 7.80 (s, 1H), 7.22 (d, 1H, *J* = 8.8), 6.91 (d, 2H, *J* = 9.2), 4.52 (s, 1H, 17.6), 3.85 (s, 3H), 3.84 (d, 1H, 17.6), 3.14 (s, 3H). Anal. Calcd for $C_{18}H_{15}Cl_2NO_4$: C, 56.86; H, 3.98; N, 3.68. Found: C, 56.75; H, 3.97; N, 3.70.

4,7-Dichloro-1-methylindoline-2,3-dione (13). To a solution of 4,7-dichloroisatin (500 mg, 2.31 mmol) in DMF at 0 °C was added sodium hydride (110 mg, 4.62 mmol). The mixture was stirred for 30 min followed by dropwise addition of methyl iodine (215 μL, 3.46 mmol). The reaction was monitored by TLC, quenched with ammonium chloride, extracted with ethyl acetate, washed with brine, dried over sodium sulfate, and purified with flash chromatography, eluting with hexane/ethyl acetate to afford **13**; yield (54.51%) 290 mg. ¹H NMR (CDCl₃, 400 Hz) δ 7.45 (d, 1H, *J* = 8.8), 7.02 (d, 1H, *J* = 8.8), 3.65 (s, 3H).

Synthesis of 4,7-Dichloro-3-methoxy-3-(2-(4-methoxyphenyl)-2-oxoethyl)indolin-2-one (14a). Compound **14a** was prepared via general procedure B from **13a** (75 mg, 0.33 mmol) and **7a** (195.8 mg, 1.31 mmol) to yield a white solid (109.4 mg, 91.4%); mp 158.5–159 °C. ¹H NMR (DMSO-*d*₆, 400 Hz) δ 7.88 (d, 2H, *J* = 8.8), 7.32 (d, 1H, *J* = 8.8), 7.01 (d, 2H, *J* = 8.8), 6.96 (d, 1H, *J* = 8.8), 6.44 (s, 1H), 4.45 (d, 1H, *J* = 18), 3.82 (s, 3H), 3.70 (d, 1H, *J* = 18), 3.48 (s, 3H). ¹³C NMR (DMSO-*d*₆, 100 Hz) δ 195.2, 177.04, 164.02, 142.4, 132.9, 130.8 (2C), 130.4, 129.02, 128.8, 124.64, 114.5 (2C), 113.6, 73.6, 56.05, 44.7, 29.87. HRMS (ES) *m/z* calcd for $C_{18}H_{15}Cl_2NO_4$ ($M + H$)⁺ 380.0456; found, 380.0441. Anal. Calcd for $C_{18}H_{15}Cl_2NO_4$: C, 56.86; H, 3.98; N, 3.68. Found: C, 56.74; H, 4.01; N, 3.64.

4,7-Dichloro-3-hydroxy-3-(2-(4-methoxyphenyl)-2-oxoethyl)-1-phenylindolin-2-one (14b). Compound **14b** was prepared via

general procedure B from *N*-benzyl-4,7-dichloroisatin (100 mg, 0.33 mmol) and **7a** (202 mg, 1.31 mmol) to yield a white solid (152 mg, 100%); mp 154–156 °C. ¹H NMR (DMSO-*d*₆, 400 MHz) δ 7.94 (d, 2H, *J* = 8.8 Hz), 7.56 (d, 2H, *J* = 8.8 Hz), 7.30 (m, 4H), 7.25 (d, 2H, *J* = 8.8 Hz), 6.98 (d, 1H, *J* = 8.8 Hz), 6.68 (s, 1H), 5.22 (s, 2H), 4.49 (d, 1H, *J* = 18.4 Hz), 3.84 (d, 1H, *J* = 18.4 Hz). Anal. Calcd for C₂₃H₁₆Cl₃NO₃: C, 59.96; H, 3.50; N, 3.04. Found: C, 59.96, H, 3.48, N, 3.01.

Synthesis of 4,7-Dichloro-3-methoxy-3-(2-(4-methoxyphenyl)-2-oxoethyl)-1-methylindolin-2-one (15). To a solution of **14a** (75 mg, 0.20 mmol) in THF (5 mL) was added MeI (127 μL) at rt. The mixture was treated with 1.6 mmol of Ag₂O (86.3 mg, 0.33 mmol). The progress of reaction was monitored by TLC (12 h). When complete, the reaction mixture was filtered over Celite. The filtrate was washed with saturated solutions of sodium sulfite, sodium bicarbonate, and brine, dried, and evaporated. The residue was purified on silica gel column using hexane/EtOAc (9:1) as an eluent to afford a white solid (46.5 mg, 57%); mp 152–153 °C. ¹H NMR (DMSO-*d*₆, 400 Hz) δ 7.64 (d, 2H, *J* = 8.8), 7.12 (d, 1H, *J* = 8.8), 6.82 (d, 2H, *J* = 7.6), 6.79 (d, 1H, *J* = 8.8), 4.45 (d, 1H, *J* = 18), 3.76 (s, 3H), 3.70 (d, 1H, *J* = 20.4), 3.60 (s, 3H), 2.97 (s, 3H). ¹³C NMR (DMSO-*d*₆, 100 Hz) δ 194.68, 174.77, 164.14, 143.11, 134.09, 130.92 (2C), 129.61, 128.76, 125.49, 124.92, 114.51 (2C), 114.16, 79.93, 56.08, 51.85, 44.35, 29.98. HRMS (ES) *m/z* calcd for C₁₉H₁₇Cl₂NO₄ (M + H)⁺ 426.0300; found 426.0306. Anal. Calcd for C₁₉H₁₇Cl₂NO₄: C, 57.88; H, 4.35; N, 3.55. Found, C, 57.62; H, 4.49; N, 3.56.

1-(6-Methoxypyridin-3-yl)ethanol. To a suspension of 5-bromo-2-methoxypyridine (206 μL, 1.59 mmol) in THF (5 mL) was added *n*-BuLi in hexane (702 μL, 1.75 mmol) dropwise over 15 min at –78 °C. The mixture was stirred for 1 h at –78 °C, and to the resulting solution was added acetaldehyde (98 μL, 1.75 mmol). The mixture was stirred for 2 h at –78 °C and then warmed to rt over 40 min. The reaction mixture was quenched with cold water, and the aqueous layer was extracted with Et₂O (3 × 35 mL). The combined organic layers were washed with brine and were dried over Na₂SO₄ and concentrated under pressure. Purification of the semisolid residue by silica gel chromatography (hexane/EtOAc) afforded a white solid (180 mg, 73.67%). ¹H NMR (CDCl₃, 400 Hz) δ 8.83 (d, 1H, *J* = 8.4), 8.74 (d, 1H, *J* = 8), 8.07 (dd, 1H), 5.16 (dd, 1H), 4.07 (s, 3H), 3.25 (s, 3H).

1-(6-Methoxypyridin-3-yl)ethanone (17). To a suspension of newly synthesized 1-(6-methoxypyridin-3-yl)ethanol (150 mg, 0.97 mmol) in CH₂Cl₂ (5 mL) were added pyridium dichloromate (733 mg, 1.95 mmol) and 4 Å molecular sieve (100 mg) at 0 °C. The mixture was stirred at 0 °C and monitored with TLC. Upon the completion of the reaction, the reaction mixture was filtered and washed with DCM. The filtered solution was washed with brine and dried over Na₂SO₄ and concentrated under pressure. Purification of the semisolid residue by silica gel chromatography (hexane/EtOAc) afforded a white solid (90 mg, 61%). ¹H NMR (CDCl₃, 400 Hz) δ 8.75 (s, 1H), 8.12 (d, 1H, *J* = 10.8), 6.77 (d, 1H, *J* = 8.8), 3.98 (s, 3H), 2.54 (s, 3H).

Synthesis of 4,7-Dichloro-3-hydroxy-3-(2-(6-methoxypyridin-3-yl)-2-oxoethyl)indolin-2-one (18). Compound **18** was prepared via general procedure B from 4,7-dichloroisatin (65 mg, 0.3 mmol) and **17** (90 mg, 0.595 mmol) to yield a white solid (79.8 mg, 72.45%); mp 203–204 °C. ¹H NMR (DMSO-*d*₆, 400 MHz) δ ppm 10.98 (s, 1H), 8.85 (s, 1H), 8.12 (dd, 1H, *J* = 11.2), 7.31 (d, 1H, *J* = 8.8), 6.91 (dd, 2H, *J* = 10.8), 6.45 (s, 1H), 4.37 (d, 1H, *J* = 18), 3.94 (s, 3H), 3.72 (d, 1H, *J* = 18). ¹³C NMR (DMSO-*d*₆, 100 Hz): 194.9, 177.8, 166.9, 149.7, 143.03, 138.8, 130.9, 129.7, 128.7, 126.1, 123.7, 113.3, 111.3, 75.0, 54.5, 44.6. HRMS (ES) *m/z* calcd for C₁₆H₁₂Cl₂N₂O₄ (M + H)⁺ 367.0252; found, 367.0235. Anal. Calcd for C₁₆H₁₂Cl₂N₂O₄·0.1EtOAc: C, 52.39; H, 3.43; N, 7.45. Found: C, 52.51; H, 3.4; N, 7.58.

5-(tert-Butoxycarbonylamino)pentanoic Acid (20). To a solution of 6-aminohexanoic acid (10 g, 76.23 mmol) in dry MeOH (90 mL) were added TEA (15.94 mL) and Boc₂O (19.96 g, 91.47 mmol). The reaction mixture was reflux at 60 °C overnight. Subsequently the reaction mixture was washed with 2 N HCl and

the pH was adjusted to 4 and extracted with ethyl acetate (3 × 75 mL). The combined organic extracts were washed with 1 N aqueous NaOH (3 × 75 mL) followed by extraction with ethyl acetate. The aqueous layer was washed with 1 N HCl (3 × 100 mL) followed by extraction with ethyl acetate. The organic phase was washed with brine, dried with Na₂SO₄ and the volatiles were removed by means of a rotary evaporator to afford a colorless oil (18.67 g, 90% yield). ¹H NMR (CD₃OD, 400 MHz) δ 5.10 (s, 1H), 4.12 (dd, 1H, *J* = 21.2), 3.05 (t, 2H, *J* = 14), 2.31 (t, 2H, *J* = 14), 1.65 (m, 2H), 1.50 (m, 2H), 1.43 (s, 9H), 1.39 (m, 2H).

tert-Butyl 6-(4-Acetylphenylamino)-6-oxohexylcarbamate (21). To a solution of **20** (1.10 g, 4.75 mmol) in CH₂Cl₂ were added DCC (2.10 g, 10.19 mmol) and DMAP (166 mg, 1.36 mmol) at 0 °C with N₂ inlet. The reaction mixture was stirred for 30 min, and 4-acetyl-*N*-methylaniline (500 mg, 3.4 mmol) was subsequently added. The resulting mixture was stirred at room temperature for 12 h. The resulting mixture was filtered and concentrated and purified by silica gel chromatography (hexane/EtOAc) to afford a white solid (712 mg, 58%). ¹H NMR (CDCl₃, 400 Hz) δ 7.85 (d, 2H, *J* = 8.8), 7.12 (d, 2H, *J* = 8.8), 3.29 (s, 3H), 3.28 (s, 3H), 2.88 (t, 2H, *J* = 14), 1.97 (t, 2H, *J* = 13.2), 1.45 (m, 2H), 1.24 (s, 9H), 1.22 (m, 2H), 1.07 (m, 2H).

tert-Butyl 6-((4-(2-(4,7-Dichloro-3-hydroxy-2-oxoindolin-3-yl)acetyl)phenyl)(methyl)amino)-6-oxohexylcarbamate (22). Compound **22** was prepared via general procedure B from 4,7-dichloroisatin (143 mg, 0.55 mmol) and **21** (600 mg, 1.65 mmol) to yield a yellow solid (305 mg, 95%). ¹H NMR (400 Hz, DMSO-*d*₆) δ 10.97 (s, 1H), 7.95 (d, 2H, *J* = 8.4), 7.43 (d, 2H, *J* = 8.4), 7.29 (d, 1H, *J* = 8), 6.99 (d, 1H, *J* = 8), 6.69 (t, 1H, *J* = 10.8), 6.44 (s, 1H), 4.40 (d, 1H, *J* = 18.4), 3.73 (d, 1H, *J* = 18.4), 3.17 (s, 3H), 2.84 (q, 2H) 2.12 (t, 2H, *J* = 13.1), 1.46 (m, 2H), 1.32 (s, 9H), 1.28 (m, 2H), 1.14 (m, 2H).

7-Amino-*N*-(4-(2-(4,7-dichloro-3-hydroxy-2-oxoindolin-3-yl)acetyl)phenyl)-*N*-methylheptanamide (23). To a suspension of **22** (300 mg, 0.518 mmol) in CH₂Cl₂ (3 mL) was added TFA (1 mL), and the reaction mixture was stirred for 1.5 h at room temperature. The solvent and the TFA were removed in vacuo. The crude product was purified by silica gel chromatography (CH₂Cl₂/MeOH) to afford a yellow solid in a quantitative yield. ¹H NMR (DMSO-*d*₆, 400 Hz) δ 7.97 (d, 2H, *J* = 8.4), 7.44 (d, 2H, *J* = 8.4), 7.30 (d, 1H, *J* = 8.8), 6.89 (d, 1H, *J* = 8.8), 6.45 (s, 1H), 4.4 (d, 1H, *J* = 18.4), 3.74 (d, 1H, *J* = 18.4), 3.30 (s, 2H), 3.18 (s, 3H), 2.72 (t, 2H, *J* = 18.4), 2.12 (t, 2H, *J* = 6.8), 1.49 (m, 4H), 1.22 (m, 2H).

***N*-(4-(2-(4,7-Dichloro-3-hydroxy-2-oxoindolin-3-yl)acetyl)phenyl)-*N*-methyl-6-(5-((4*R*)-2-oxohexahydro-1*H*-thieno[3,4-*d*]imidazol-4-yl)pentanamido)hexanamide (24).** To a solution of biotin (66.5 mg, 0.27 mmol) in DCM were added EDCl-HCl (52.2 mg, 0.27 mmol) and HOBt (41.7 mg, 0.27 mmol). After stirring at rt for 30 min **23** (100 mg, 0.20 mmol) was added followed by DMAP (33.2 mg, 0.27 mmol). The mixture was stirred at rt for 16 h, followed by flash column purification. The resulting fractions were evaporated to afford a white powder. ¹H NMR (CD₃OD, 400 Hz) δ 11.02 (s, 1H), 8.02 (d, 2H, *J* = 8.8), 7.87 (t, 1H, *J* = 10.8), 7.41 (d, 2H, *J* = 8.8), 7.25 (d, 1H, *J* = 8.8), 6.90 (d, 1H, *J* = 8.8), 4.83 (d, 1H, *J* = 18), 4.58 (d, 1H, *J* = 18), 4.95 (q, 1H), 4.30 (dd, 1H, *J* = 12.4), 3.84 (dd, 1H, *J* = 19.6), 3.32–3.30 (m, 2H), 3.27 (s, 3H), 3.20–3.15 (m, 1H), 3.13 (q, 2H), 2.92 (dd, dd, 1H), 2.7 (d, 1H, *J* = 12.8), 2.18 (t, 4H, *J* = 14.4), 1.74–1.63 (m, 2H), 1.59–1.55 (m, 4H), 1.44–1.36 (m, 4H), 1.28–1.77 (m, 2H). ¹³C NMR (CD₃OD, 100 Hz) δ 195.68, 178.39, 174.50, 173.60, 164.6, 148.40, 142.33, 130.41 (2C), 129.34, 128.92, 128.64, 127.23, 123.57 (2C), 113.79, 75.10, 61.98, 60.21, 55.57, 44.18, 39.64, 38.78, 38.66, 36.29, 35.41, 33.56, 28.64, 28.33, 28.07, 26.02, 25.50, 24.72. Anal. Calcd for C₃₃H₃₉Cl₂N₅O₆S: C, 56.25; H, 5.58; N, 9.94. Found: C, 56.20; H, 5.61; N, 9.98.

X-ray Crystallography. Single crystals of **10** were grown by slow evaporation from ethyl acetate. Single crystal diffraction data were collected at 223(2) K on a Bruker APEX II CCD X-ray diffractometer equipped with a 700 Series Oxford Cryostream low temperature device and employing Mo K α radiation (0.710 73 Å). Notably, initial attempts to collect data at 100(2) K were unsuccessful because of deterioration of the crystals at this temperature, presumably the result

of a temperature-induced phase change. The structure was solved by direct methods using SHELXS, and all structural refinements were conducted using SHELXL-97-2.²⁹ All non-hydrogen atoms were modeled with anisotropic displacement parameters. All hydrogen atoms were located in the final difference Fourier map and were refined, without restraints, with isotropic displacement parameters. The program X-Seed was used as a graphical interface for the SHELX software suite and for the generation of figures.³⁰ CCDC-988096 contains the supplementary crystallographic data. These data can be obtained free of charge via <http://www.ccdc.cam.ac.uk/conts/retrieving.html> or from The Cambridge Crystallographic Data Centre, 12 Union Road, Cambridge, CB2 1EZ, U.K.; fax, (+44) 1223-336-033; e-mail, deposit@ccdc.cam.ac.uk.

Biological Evaluation. Cell Culture. TC32, TC71 cells were grown in RPMI with 10% fetal bovine serum (FBS) and 1% HEPES. PANC1 and COS7 cells were grown in DMEM with 10% FBS. Cells were grown at 37 °C in humidified atmosphere of 5% CO₂ in a VWR CO₂ incubator.

Cell Proliferation Assays. The effect of the new derivatives on TC32, TC71, and Panc1 cell viability were assessed. Cells were grown in colorless media and plated at a density of 5000–15000 cells/well, depending on cell line, in a 96-well plate. Analogs or vehicle alone (DMSO) was added to cells in appropriate growth media the day after plating. Viable cells were quantified using MTT or WST-1 per the manufacturer's protocol after 3 days of treatment. GI₅₀ values were calculated by nonlinear regression analysis using GraphPad Prism 4.0.

Reporter Assay. EWS-FLI1 activity was assessed using NROB1 luciferase construct containing EWS-FLI1 binding sites. COS7 cells were transiently transfected with NROB1 luciferase reporter and full length EWS-FLI1 or empty vector control (pCI-neo-EV) with Xtremegene 9 (Roche) according to the manufacturer's protocol. One and half hours after transfection, cells were treated with 0.05, 0.15, 0.5, 1.5, 5, and 15 μM appropriate compounds or DMSO. Luciferase activity was measured 20 h after treatments. All the luciferase assays were performed using a luciferase assay kit according to the manufacturer's protocol (Promega). IC₅₀ values were calculated by sigmoidal dose–response curve fit using GraphPad Prism 4.0.

Protein Purification. EWS-FLI1 was expressed in BL21 cells to an OD of 0.6–0.8 and induced with 1 mM IPTG. Following 2 h of shaking at 27 °C, the protein was pelleted by centrifugation at 9500 rpm. The inclusion bodies were treated with Bugbuster (Novagen) following the manufacturer's instructions. The resulting pellet was denatured in binding buffer containing 20 mM Tris-HCl, 500 mM NaCl, 6 M guanidinium, and 50 mM imidazole, pH 7.4, and filtered through a 0.22 μm filter. Protein was loaded on a HiTrap chelating HP column (GE) that is precharged with 0.1 M NiSO₄ and subject to purification on AKTA explorer or AKTA purifier system. Protein was loaded on the column at 0.5 mL/min and washed with buffer contain 20 mM Tris-HCl, 500 mM NaCl, 8 M urea, and 50 mM imidazole. Next, the protein on the column was refolded using a slow gradient to a buffer containing 20 mM Tris-HCl, 500 mM NaCl, and 50 mM imidazole at 0.5 mL/min. Column elution done in a buffer containing 2 M imidazole was performed with the protein eluting in fractions equivalent to 1.2 M imidazole.

Binding Assay. A 96-well plate (Maxisorb) was coated with 100 μL of recombinant EWS-FLI1 overnight at a concentration of 20 nM per well. Coated wells were blocked with 150 μL of 4% bovine albumin serum (BSA) in PBS at for 1 h at room temperature. The biotin conjugate **24** was diluted from stock DMSO in assay buffer (A15). After washing the conjugate was added to each well and incubated for 1 h. The complex was washed five times in a washing buffer followed by the incubation of 1:5000 dilution of HRP-streptavidin (Thermo Scientific, N100) for 1 h at room temperature. After washing five times, the bound biotin conjugate was detected using the colorimetric phosphatase substrate. After development, the absorbance was measured at 405 nm. The data were analyzed using GraphPad Prism.

AUTHOR INFORMATION

Corresponding Author

*(M.L.B.): Phone: +1-202-687-8603. Fax: +1-202-687-7659. Email: mb544@georgetown.edu.

Notes

The authors declare the following competing financial interest(s): P.N.T., Y.K., A.U., J.T., and M.L.B. are co-inventors on the following patent: PCT/US2013/036234.

ACKNOWLEDGMENTS

We thank the Center for Drug Discovery at Georgetown University for support. We also acknowledge the Lombardi Comprehensive Cancer Center Biocore Shared Resource, which is partially supported by NIH/NCI Grant P30-CA051008. This research was supported by NIH Grants R01 CA138212, R01 CA133662, and RC4 CA156509. We are grateful to the Department of Chemistry of the George Washington University for use of their diffractometer.

ABBREVIATIONS USED

ESFT, Ewing's sarcoma family tumors; ES, Ewing's sarcoma; ETS, E26 transformation-specific; FLI1, friend leukemia 1; IDP, intrinsically disordered protein; RHA, RNA helicase A; *n*-BuLi, *n*-butyllithium; PDC, pyridinium dichromate; DCC, *N,N'*-dicyclohexylcarbodiimide; EDCI, 1-ethyl-3-(3-dimethylaminopropyl)carbodiimide; WST, water-soluble tetrazolium

REFERENCES

- (1) Wexler, L. H.; DeLaney, T. F.; Tsokos, M.; Avila, N.; Steinberg, S. M.; Weaver-McClure, L.; Jacobson, J.; Jarosinski, P.; Hijazi, Y. M.; Balk, F. M.; Horowitz, M. E. Ifosfamide and Etoposide plus Vincristine, Doxorubicin, and Cyclophosphamide for Newly Diagnosed Ewing's Sarcoma Family of Tumors Leonard. *Cancer* **1996**, *78*, 901–911.
- (2) Suvà, M.-L.; Riggi, N.; Stehle, J.-C.; Baumer, K.; Tercier, S.; Joseph, J.-M.; Suvà, D.; Clément, V.; Provero, P.; Cironi, L.; Osterheld, M.-C.; Guillou, L.; Stamenkovic, I. Identification of Cancer Stem Cells in Ewing's Sarcoma. *Cancer Res.* **2009**, *69*, 1776–1781.
- (3) Kovar, H. Context Matters: The Hen or Egg Problem in Ewing's Sarcoma. *Semin. Cancer Biol.* **2005**, *15*, 189–196.
- (4) Wilkins, R. M.; Pritchard, D. J.; Burgert, O. J. E.; Unni, K. K. Ewing's Sarcoma of Bone. *Cancer* **1986**, *58*, 2551–2555.
- (5) Grier, H. E.; Krailo, M. D.; Tarbell, N. J.; Link, M. P.; Fryer, C. J. H.; Pritchard, D. J.; Gebhardt, M. C.; Dickman, P. S.; Perlman, E. J.; Meyers, P. a; Donaldson, S. S.; Moore, S.; Rausen, A. R.; Vietti, T. J.; Miser, J. S. Addition of Ifosfamide and Etoposide to Standard Chemotherapy for Ewing's Sarcoma and Primitive Neuroectodermal Tumor of Bone. *N. Engl. J. Med.* **2003**, *348*, 694–701.
- (6) Ginsberg, J. P.; de Alava, E.; Ladanyi, M.; Wexler, L. H.; Kovar, H.; Paulussen, M.; Zoubek, A.; Dockhorn-Dworniczak, B.; Juergens, H.; Wunder, J. S.; Andrulis, I. L.; Malik, R.; Sorensen, P. H. B.; Womer, R. B.; Barr, F. G. EWS-FLI1 and EWS-ERG Gene Fusions Are Associated with Similar Clinical Phenotypes in Ewing's Sarcoma. *J. Clin. Oncol.* **1999**, *17*, 1809–1814.
- (7) Arvand, A.; Denny, C. T. Biology of EWS/ETS Fusions in Ewing's Family Tumors. *Oncogene* **2001**, *20*, 5747–5754.
- (8) Delattre, O.; Zucman, J.; Plougastel, B.; Desmaze, C.; Melot, T.; Peter, M.; Kovar, H.; Joubert, I.; de Jong, P.; Rouleau, G.; Aurias, A.; Thomas, G. Gene Fusion with an ETS DNA-Binding Domain Caused by Chromosome Translocation in Human Tumours. *Nature* **1992**, *359*, 162–165.
- (9) May, W. A.; Gishizky, M. L.; Lessnick, S. L.; Lunsford, L. B.; Lewis, B. C.; Delattre, O.; Zucman, J.; Thomas, G.; Denny, C. T. Ewing Sarcoma 11;22 Translocation Produces a Chimeric Tran-

scription Factor That Requires the DNA-Binding Domain Encoded by FLI1 for Transformation. *Proc. Natl. Acad. Sci. U.S.A.* **1993**, *90*, 5752–5756.

(10) Hu-Lieskovan, S.; Heidel, J. D.; Bartlett, D. W.; Davis, M. E.; Triche, T. J. Sequence-Specific Knockdown of EWS-FLI1 by Targeted, Nonviral Delivery of Small Interfering RNA Inhibits Tumor Growth in a Murine Model of Metastatic Ewing's Sarcoma. *Cancer Res.* **2005**, *65*, 8984–8992.

(11) Wright, P. E.; Dyson, H. J. Intrinsically Unstructured Proteins: Re-Assessing the Protein Structure-Function Paradigm. *J. Mol. Biol.* **1999**, *293*, 321–331.

(12) Ng, K. P.; Potikyan, G.; Savene, R. O. V.; Denny, C. T.; Uversky, V. N.; Lee, K. A. W. Multiple Aromatic Side Chains within a Disordered Structure Are Critical for Transcription and Transforming Activity of EWS Family Oncoproteins. *Proc. Natl. Acad. Sci. U.S.A.* **2007**, *104*, 479–484.

(13) Erkizan, H. V.; Uversky, V. N.; Toretsky, J. A. Oncogenic Partnerships: EWS-FLI1 Protein Interactions Initiate Key Pathways of Ewing's Sarcoma. *Clin. Cancer Res.* **2010**, *16*, 4077–4083.

(14) Darnell, J. E. Transcription Factors as Targets for Cancer Therapy. *Nat. Rev. Cancer* **2002**, *2*, 740–749.

(15) Bhalla, J.; Storchan, G. B.; MacCarthy, C. M.; Uversky, V. N.; Tcherkasskaya, O. Local Flexibility in Molecular Function Paradigm. *Mol. Cell. Proteomics* **2006**, *5*, 1212–1223.

(16) Toretsky, J. A.; Erkizan, V.; Levenson, A.; Abaan, O. D.; Parvin, J. D.; Cripe, T. P.; Rice, A. M.; Lee, S. B.; Uren, A. Oncoprotein EWS-FLI1 Activity Is Enhanced by RNA Helicase A. *Cancer Res.* **2006**, *66*, 5574–5581.

(17) Erkizan, H. V.; Kong, Y.; Merchant, M.; Schlottmann, S.; Barber-Rotenberg, J. S.; Yuan, L.; Abaan, O. D.; Chou, T.-H.; Dakshanamurthy, S.; Brown, M. L.; Uren, A.; Toretsky, J. A. A Small Molecule Blocking Oncogenic Protein EWS-FLI1 Interaction with RNA Helicase A Inhibits Growth of Ewing's Sarcoma. *Nat. Med.* **2009**, *15*, 750–756.

(18) Barber-Rotenberg, J. S.; Selvanathan, S. P.; Erkizan, H. V.; Snyder, T. M.; Hong, S. P.; Kobs, C. L.; South, N. L.; Summer, S.; Monroe, P. J.; Chruszcz, M.; Dobrev, V.; Tosso, P. N.; Scher, L. J.; Minor, W.; Brown, M. L.; Metallo, S. J.; Uren, A.; Toretsky, J. A. Single Enantiomer of YK-4-279 Demonstrates Specificity in Targeting the Oncogene EWS-FLI1. *Oncotarget* **2012**, *3*, 172–182.

(19) Dunker, A. K.; Uversky, V. N. Drugs for “Protein Clouds”: Targeting Intrinsically Disordered Transcription Factors. *Curr. Opin. Pharmacol.* **2010**, *10*, 782–788.

(20) Uren, A.; Toretsky, J. A. Ewing's Sarcoma Oncoprotein EWS-FLI1: The Perfect Target without a Therapeutic Agent. *Futur. Oncol.* **2005**, *1*, 521–528.

(21) Marvel, C. S.; Hiers, G. S. Isatin. *Org. Synth., Collect. Vol.* **1941**, *1*, 327.

(22) Li, S.; Huang, Q.; Liu, Y.; Zhang, X.; Liu, S.; He, C.; Gong, P. European Journal of Medicinal Chemistry Design, Synthesis and Antitumour Activity of Bisquinoline Derivatives Connected by 4-Oxy-3-Fl Uoroaniline Moiety. *Eur. J. Med. Chem.* **2013**, *64*, 62–73.

(23) Braude, F.; Lindwall, H. G. Condensations of Isatin with Acetone by the Knoevenagel Method. *J. Am. Chem. Soc.* **1933**, *55*, 325–327.

(24) Lopez-Alvarado, P.; Avendaño, C. New Diastereoselective Synthesis of 3-Alkylidene-1-Methyloxindoles. *Synthesis* **2002**, *1*, 104–110.

(25) Bissantz, C.; Kuhn, B.; Stahl, M. A Medicinal Chemist's Guide to Molecular Interactions. *J. Med. Chem.* **2010**, *53*, 5061–5084.

(26) Al-Tel, T. H. Design, Synthesis and Qualitative Structure–Activity Evaluations of Novel Hexahydropyrano[3,2-*c*][1,2]diazepin-3(4*H*)-one and Tetrahydropyrano[3,2-*b*]pyrrol-2(1*H*)-one Derivatives As Anticancer Agents. *Eur. J. Med. Chem.* **2010**, *45*, 4615–4621.

(27) Kinsey, M.; Smith, R.; Iyer, A. K.; McCabe, E. R. B.; Lessnick, S. L. EWS/FLI and Its Downstream Target NR0B1 Interact Directly To Modulate Transcription and Oncogenesis in Ewing's Sarcoma. *Cancer Res.* **2009**, *69*, 9047–9055.

(28) Gangwal, K.; Lessnick, S. L. Microsatellites Are EWS/FLI Response Elements: Genomic “Junk” Is EWS/FLI's Treasure. *Cell Cycle* **2008**, *7*, 3127–3132.

(29) Sheldrick, G. M. A Short History of SHELX. *Acta Crystallogr., Sect. A* **2008**, *64*, 112–122.

(30) Barbour, L. J. X-Seed—A Software Tool for Supramolecular Crystallography. *J. Supramol. Chem.* **2001**, *1*, 189–191.